Cost-effective transformation of a Highly-Efficient Advanced Thermal Ultra-SuperCritical coal-fired power plant into a CHP by retrofitting and integrating an ARBAFLAME biomass upgrading process

D1.4 MAPPING, CHARACTERIZATION AND CRITICAL EVALUATION OF THE STATE-OF-THE-ART

Deliverable information

Deliverable no.:	D1.4
Work package no.:	1
Document version:	V.4
Document Preparation Date:	30.12.2019
Responsibility:	Partner No. 5 – SINTEF

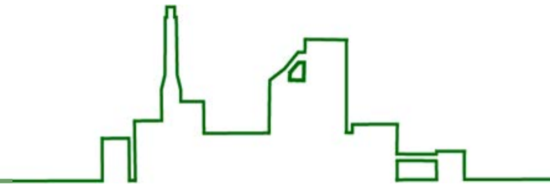

This project has received funding from the European Union's Horizon 2020 research and innovation programme under grant agreement No 818349

This project has received funding from the European Union's Horizon 2020 research and innovation programme under grant agreement No 818349

Version management		
Filename:		D1.4_Mapping, characterization and critical evaluation of the state-of-the-art.doc
Author(s):		Gonzalo del Alamo, Olaf Lehn Tranås (SINTEF)
Reviewed by:		Øyvind Skreiberg (SINTEF)
Approved by:		Marijn Mulder (PNO)
Revision no.	**Date**	**Modification description**
RV.1	15.11.2019	First draft
RV.2	26.11.2019	Final version for internal QA at SINTEF
RV.3	10.12.2019	Revised version after internal QA at SINTEF, including preliminary value chain results
RV.4	30.12.2019	Revised version after external QA from PNO, including data for fast pyrolysis as an alternative pretreatment technology

Dissemination level		
PU	Public	X
CO	Confidential, only for Members of the Consortium, including the EU Commission Services	

Type of deliverable		
R	Document, report, drawings	X
DEM	Demonstrator, pilot, prototype	
DEC	Website, patent filings, video’s, etc	
OTHER		
ETHICS	Ethics requirements	

This project has received funding from the European Union’s Horizon 2020 research and innovation programme under grant agreement No 818349

Project information	
Project acronym	ARBAHEAT
EC Grant Agreement no.:	818349
Project Coordinator:	PNO
Project start date:	01.10.2018
Duration:	48 months

TABLE OF CONTENTS

This project has received funding from the European Union's Horizon 2020
research and innovation programme under grant agreement No 818349

This project has received funding from the European Union’s Horizon 2020 research and innovation programme under grant agreement No 818349

LIST OF ACRONYMS AND ABBREVIATIONS

CA: Consortium Agreement

CO: Confidential

DoW: Description of Work, referring to the Annex I of the Grant Agreement

EC: European Commission

GA: Grant Agreement

IPR: Intellectual Property Rights

PU: Public

QA: Quality Assurance

WP: Work Package

EXECUTIVE SUMMARY

The ARBAHEAT demonstration project addresses the co-firing of steam-exploded biomass into an existing pulverized-coal combustion (PCC) plant with production of power and heat. This deliverable focuses on establishing a mathematical framework for the complete value chain evaluation and reviewing the current state-of-the-art for the main aspects of the value chain affecting the process, including economics and environmental performance.

The main aspects of the value chain that have been considered include:

1. The geographical and time distribution of the availability of the biomass raw feedstock
2. Energy consumption, greenhouse gas (GHG) emissions and cost of transport of woody biomass for large-scale centralized co-firing
3. Process and environmental performance of the mechanical and thermochemical treatment of woody biomass
4. Process and environmental performance of co-firing steam-exploded biomass into the PCC plant.

Evaluation of the geographical and time distribution of the availability of the feedstock has been performed based on overall balances between the available forest wood and other renewable biomass resources and waste and the total demand of renewable resources to the overall energy sector using available data from the European statistical database (Eurostat) and the literature. The total cost, energy consumption and emissions for collecting and transporting the feedstock along the value chain consider both single-mode and inter-mode depending on the capacity of the PCC plant and the distribution of the availability of the feedstock. Calculation of the transport cost includes both internal costs, related to the capital investment and the operating cost depending on the transport time and distance, and external cost related to the impact of transport on infrastructure, environment and human health.

The state-of-the-art production of black pellets via steam explosion of woody biomass has been reviewed and compared with alternative thermochemical treatment of woody biomass. The main aspects considered when reviewing the state-of-the-art include: 1) Mapping the yield, composition and key properties of the solid product as a function of the operational parameters for both softwood and hardwood, and 2) overall process design and associated mass and energy flows for the overall conversion of the raw feedstock to black pellets. The steam explosion technology has been benchmarked with other relevant technological routes enabling the co-firing of woody biomass into pulverized-coal power plants, i.e. torrefaction, hydrothermal carbonization and fast pyrolysis. Co-firing of black pellets in the PCC plant has been reviewed, focusing on the following aspects: 1) safety issues during handling and storage of biomass, 2) slagging, fouling and corrosion problems, and 3) overall process performance of the PPC plant as a function of co-firing ratio.

A preliminary evaluation of the overall energy efficiency, GHG emissions and the economics along the complete value chain has been performed.

This project has received funding from the European Union's Horizon 2020
research and innovation programme under grant agreement No 818349

1. Introduction

1.1 Objectives of this deliverable

The overall objective of the ARBAHEAT project is to demonstrate the technical and economic feasibility of co-firing steam-exploded (SE) biomass into an existing pulverized-coal combustion (PCC) plant with production of power and heat based on supercritical steam conditions. The SE plant is based on the proprietary technology of Arbaflame. The PCC plant is owned by ENGIE and located in the Maasvlakte industrial area in Rotterdam (The Netherlands).

The specific objectives of this deliverable are:

1. Establish a framework to evaluate the overall process, economic and environmental performance of the value chain.
2. Review the updated trends for the geographical, across Europe, and time-dependent availability of woody biomass feedstock in Europe up to 2050.
3. Review the current state-of-the-art and overall performance of the production of black pellets from steam-explosion of woody biomass and compare with alternative pre-treatment technologies.
4. Review the main process and operational aspects of co-firing SE pellets into the PCC plant.
5. Perform a preliminary evaluation of the overall process, GHG emissions and economic performance of the value chain.

1.2 Background information and assumptions

This report has used the following information generated within the project:

1. General objectives, technological options and process performance targets from the proposal SEP-210495257, "ARBAHEAT: Cost-effective transformation of a Highly-Efficient, Advanced, Thermal Ultra-SuperCritical coal-fired power plant into a CHP by retrofitting and integrating an ARBAFLAME biomass upgrading process."
2. M. Cieplik, "Technical requirements of the steam exploded pellets produced and fired within the integrated ENGIE-ARBAKIT system," Report ARBAHEAT/D1.2, 2019.
3. C. Stellaard and T. Maertens, "Design requirements for the cost-effective retrofit of the coal-fired power plant," Report ARBAHEAT/D1.5, 2019.

This project has received funding from the European Union's Horizon 2020 research and innovation programme under grant agreement No 818349

1.3 Symbology

Table 1: Symbology description

Symbol	**Description**
Flow variables	
$\dot{M}, \dot{V}, \dot{V}_N$	Mass flow rate, volumetric flow rate, normal volumetric flow rate
Y, X, ϕ	Mass fraction, mole fraction, volume fraction
$\dot{H}, \dot{H}_T , \dot{H}_F$	Rate of total, thermal and formation enthalpy
$\dot{Q}$	Heat flow
$\dot{W}_{el}$	Electric power
h, h_T, h_F	Specific total, thermal and formation enthalpy per unit mass
$\bar{h}, \bar{h}_T, \bar{h}_F$	Specific total, thermal and formation enthalpy per unit mole
ρ, k, μ	Bulk density, thermal conductivity and viscosity
c, c_P	Specific heat, specific heat at constant pressure
Subscripts	
B_i	Biomass feedstock
C	Coal
c_i	Consumable
w	Process water
r_i	Solid residue
el	Electricity
g	Flue gas emitted to air
th	Thermal
Superscripts	
SRC	Feedstock source
PR	Feedstock pretreatment
PCC	Pulverized-coal combustion plant
EX	Extraction of raw feedstock (woody biomass or coal) from source
EXP	Exported energy from PCC plant
MT_i	Mechanical treatment process

2. Value chain framework

2.1 Generic value chain model

Figure 1 shows a schematic representation of the value chain model considered in the ARBAHEAT project, together with the main material and energy flows. The value chain entails the co-firing of black pellets produced from steam explosion of lignocellulosic biomass into a pulverized-coal combustion plant (PCC) for production of heat and power. Firstly, the lignocellulosic biomass requires mechanical treatment to achieve a particle size distribution (PSD) suitable for the steam explosion process. The solid product from the steam explosion plant is then pelletized in order to reduce the risk of dust formation and explosion during handling and storage. Co-feeding of the steam exploded pellets is performed by direct milling with the coal before injection in the combustion chamber. The PCC plant is connected to electric and thermal grids. The steam explosion plant includes separation and recovery of condensable chemicals from the resulting vapour phase, which is sold as a by-product.

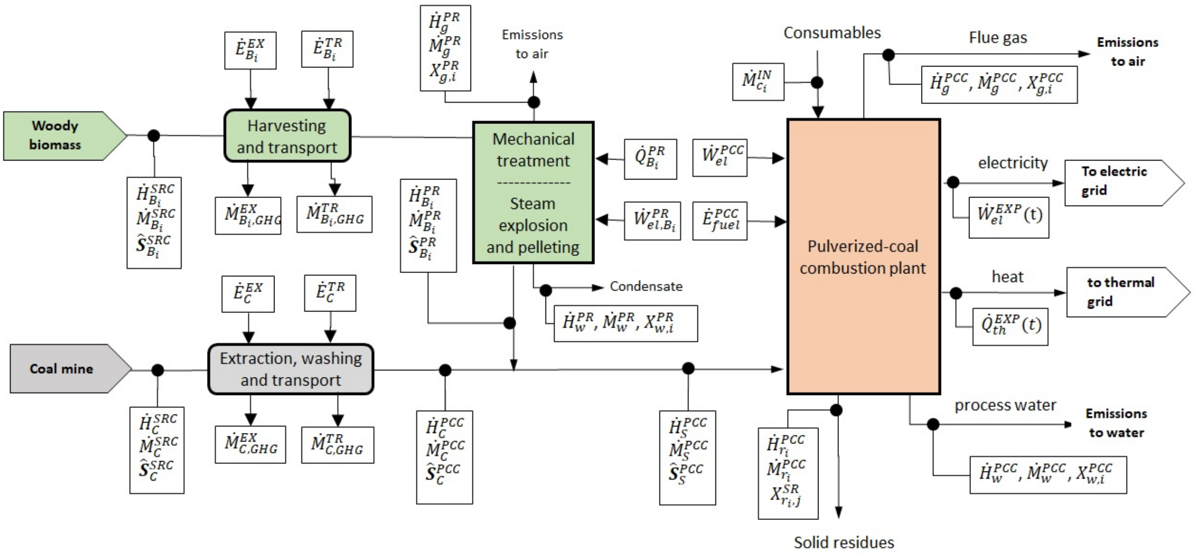

Figure 1: Schematic representation of the overall value chain considered in the ARBAHEAT project, which entails co-firing of black pellets produced from steam explosion of lignocellulosic biomass into a pulverized-coal combustion plant

2.2 Overall value chain parameters

The mathematical description of the value chain model is formulated in terms of the parameters listed in Table 2. The raw biomass feedstocks considered includes multiple sources of hardwood and softwood extracted from forests. The availability of forest wood is assumed to be dependent on the geographical location and the operating year within the timeframe 2020-2050. This timeframe considers the lifetime of both the SE and the retrofitted PCC plants. The forest is modelled as a distributed source characterized by the total surface area S_j, the mass of wood available per unit surface and unit time $\dot{m}_{B_i,S}(t)$ and characterization vector $\hat{S}_{B_i}^{SRC}$ defining the composition and physical properties of the wood as defined in Table 3. The total mass of feedstock available per unit time is calculated by integrating over the entire forest surface area from $\dot{M}_{B_i}^{SRC}(t) = \int_{S_j} \dot{m}_{B_i,S}(t) f_{B_i}(t) dS$, where $f_{B_i}(t)$ represents the availability of woody biomass for one specific source that can be used for the value chain considered in this project. The supply of forest wood from each source includes harvesting of wood from the forest, delivery at road and transport from the source to the PCC plant site. The energy and GHG emissions associated with harvesting and transport of each biomass feedstock source are denoted by $\dot{E}_{B_i}^{EX}$, $\dot{M}_{GHG,B_i}^{EX}$, $\dot{E}_{B_i}^{TR}$ and $\dot{M}_{GHG,B_i}^{TR}$. The supply chain of coal include extraction, washing and transport from point sources characterized by the total mass of feedstock available per unit time and the transport distance to the plant, denoted by $\dot{M}_{C}^{SRC}(t)$ and L_{C}^{SRC}. The energy and GHG emissions associated with coal extraction and transport are denoted by $\dot{E}_{C}^{EX}$, $\dot{M}_{GHG,C}^{EX}$, $\dot{E}_{C}^{TR}$ and $\dot{M}_{GHG,C}^{TR}$. The overall pre-treatment of the raw biomass feedstock from each source, including both the mechanical treatment and the steam explosion plant, is described based on the mass and energy yields and the characterization vector of the solid product, denoted respectively by f_{m,B_i}^{PR}, f_{e,B_i}^{PR}, $\hat{S}_{B_i}^{PR}$ and the consumption of electricity and heat, denoted by $\dot{W}_{B_i}^{PR}$ and $\dot{Q}_{B_i}^{PR}$. The overall capacity of the PCC plant is here defined as the total input solid fuel (coal and SE biomass) power, denoted by $\dot{H}_{S}^{PCC}$. The degree of co-firing is described based on the ratio between the input energy of the pretreated biomass and the total input solid fuel energy entering the PCC plant, denoted by $\eta_B = \left(\sum_i \dot{M}_{B_i}^{PCC} LHV_{B_i}^{PCC}\right)/\dot{H}_{S}^{PCC}$. The overall energy performance of the power plant is described in terms of the electric and thermal power production efficiencies calculated from $\epsilon_{el}^{PCC} = \dot{W}_{el}^{EG}/\dot{H}_{S}^{PCC}$ and $\epsilon_{th}^{PCC} = \dot{Q}_{th}^{DH}/\dot{H}_{S}^{PCC}$. The environmental impact of the PCC plant is evaluated in terms of the mass flow rate and concentration of the flue gas emitted to air, denoted by $\dot{M}_{g}^{PCC}$ and $x_{g,i}^{PCC}$, the water emissions associated to the treated process water, denoted by $\dot{M}_{w}^{PCC}$and $x_{w,i}^{PCC}$, and the solid residues, denoted by $\dot{M}_{r_i}^{PCC}$and $x_{r_i,j}^{PCC}$ with r_i denoting each solid residue (bottom ash, fly ash and gypsum from the flue gas cleaning system. Consumables and electricity required for operation of the PCC plant are evaluated in term of the mass flow rate $\dot{M}_{C_i}^{PCC}$ and the electric power load $\dot{W}_{el}^{PCC}$, where the subscript C_i represents each specific consumable as described in Table 27 of Section 5. Based on the overall power capacity of the PCC plant, the co-firing ratio and the overall energy efficiency of the combined mechanical and thermochemical (SE) pre-treatment, the mass flow rate of each raw biomass feedstock at source is calculated from $\dot{M}_{B_i}^{SRC} = Y_{B_i}^{PCC}\eta_B\dot{H}_{S}^{PCC}/\sum\left(Y_{B_i}^{PCC} LHV_{B_i}^{PCC} f_{E,B_i}^{PR}\right)$, where $Y_{B_i}^{PCC}$ is the mass fraction of the black pellets fed into the PCC plant and produced from each biomass feedstock source B_i and f_{E,B_i}^{PR} is the overall energy yield along the overall mechanical and thermochemical (SE) pre-treatment.

Table 2: Description of the main parameters used for describing mathematically the overall value chain model

Symbol	Description
η_B	Co-firing biomass energy fraction of the total input energy to the pulverized coal boiler
$\dot{M}_{B_i}^{SRC}$	Mass flow rate of one biomass feedstock from source
$\dot{M}_{B_i}^{PCC}$	Input mass flow rate of one biomass feedstock to the PCC boiler
$Y_{B_i}^{PCC}$	Mass fraction of one biomass feedstock to the PCC boiler
$\dot{M}_{C}^{SRC}$	Mass flow rate of coal from source
$\dot{M}_{C}^{PCC}$	Input mass flow rate of coal to the PCC boiler
$\dot{M}_{S}^{PCC}$	Input mass flow rate of solid fuel mix to the PCC boiler
$\dot{H}_{s}^{PCC}$	Total input solid fuel power to the PCC boiler
$\dot{W}_{el}^{PCC}$	Electric power consumed by the PCC plant
E_{fuel}^{PCC}	Fuel consumption by auxiliary burners at the PCC plant
ϵ_{el}^{PCC}	Exported electric power production to total input solid fuel power to the PCC plant
ϵ_{th}^{PCC}	Exported thermal power production to total input solid fuel power to the PCC plant
$\dot{W}_{el}^{EXP}$	Time-dependent demand of electric power exported to the electric grid
$\dot{Q}_{th}^{EXP}$	Time-dependent demand of heat exported to the thermal grid
T_{sup}^{TG}	Supply temperature to the thermal grid
T_{ret}^{TG}	Return temperature to the thermal grid
$\hat{S}_{C}^{SRC}$	Characterization vector of coal at source
$\hat{S}_{B_i}^{SRC}$	Characterization vector of one specific biomass feedstock B_i at source
$\hat{S}_{B_i}^{PR}$	Characterization vector of one specific biomass feedstock B_i after pretreatment
$\hat{S}_{S}^{PCC}$	Characterization vector of input solid-fuel mix to the boiler
f_{m,B_i}^{PR}	Mass yield of solid product from pretreatment of one biomass feedstock
f_{e,B_i}^{PR}	Energy yield of solid product from pretreatment of one biomass feedstock
$\dot{W}_{B_i}^{PR}$	Total electric power load required by the overall pretreatment of one biomass feedstock source
$\dot{Q}_{B_i}^{PR}$	Total heat power required by the overall pretreatment of one biomass feedstock source
$\dot{E}_{B_i}^{EX}$	Total input energy (fuel or electricity) flow for extracting one type of biomass feedstock from source
$\dot{M}_{GHG,B_i}^{EX}$	Mass flow of GHG emissions (CO_2-eq) from harvesting one type of biomass feedstock from source
$\dot{E}_{B_i}^{TR}$	Total input energy flow for transporting one biomass feedstock from source to the PCC plant
$\dot{M}_{GHG,B_i}^{TR}$	Mass flow of GHG emissions (CO_2-eq) from transporting one biomass feedstock from source to the PCC plant
$\dot{E}_{C}^{SRC}$	Total input energy flow required by extracting the coal feedstock from source
$\dot{M}_{GHG,C}^{EX}$	Mass flow of GHG emissions (CO_2-eq) from extracting coal from source
$\dot{E}_{C}^{TR}$	Total input energy (fuel or electricity) flow for transporting the coal feedstock from source to the PCC plant
$\dot{M}_{GHG,C}^{TR}$	Mass flow of GHG emissions (CO_2-eq) from transporting the coal feedstock from source to the PCC plant

Table 3: Description of the main parameters included in the characterization solid feedstock (coal and biomass)

Symbol	**Description**
$f(d_p)$	Particle size distribution
ρ	Density
LHV	Lower heating value
HHV	Higher heating value
Y_K	Proximate analysis $K = DM$ (Dry matter), V (Volatile matter), FC (Fixed carbon), A (Total ash), H_2O (Moisture content)
Y_i	Atomic composition

2.3 Scope of modelling

Modelling of the value chain includes the following mains aspects:

1. The location, availability and properties of the raw feedstock at source.
2. The energy consumption, GHG emissions and cost associated with the harvesting and transport of the biomass along the complete value chain from the source to the PCC plant.
3. The energy consumption, GHG emissions and cost associated with the extracting, washing and transport of the coal from the coal mine to the PCC plant.
4. Overall material and energy flows, capital investment and operating costs for the mechanical treatment and the thermal (steam explosion) treatment as a function of the composition and properties of the raw lignocellulosic feedstock.
5. Capital investment for the retrofitting of the PCC plant to enable up to 100 % co-firing of biomass based on the total input energy into the boiler of the PCC plant.
6. Time-dependent demands of power and heat by the electric and thermal grids.
7. Overall power and heat production efficiencies, operating costs and emissions of the PCC plant as a function of the biomass to coal energy ratio, the input feedstock composition entering the boiler and the power to heat energy demands ratio.

2.4 Relevant political targets, policy framework and regulations

Share of renewable resources in the energy sector

In accordance with the European Directive 2018/2001 [1], the share of energy from renewable sources in the EU based on the gross final consumption of energy shall be at least 32 % by 2030. In multi-fuel plants using renewable and non-renewable sources, only the part of electricity, heating and cooling produced from renewable sources shall be considered. For the purpose of that calculation, the contribution of each energy source shall be calculated based on its energy content.

GHG emissions reduction

The general policy framework for climate and energy between 2020 and 2030 in the European Union aims to reduce greenhouse gas emissions by at least 40 % by 2030 compared with 1990. In accordance with European Directive 2018/2001 [1], the greenhouse gas (GHG) emission savings shall be at least 70 % for electricity, heating and cooling production from biomass fuels used in installations starting operation from 1 January 2021 until 31 December 2025, and 80 % for installations starting operation from 1 January 2026. An installation shall be considered to be in operation once the physical production of biofuels, biogas consumed in the transport sector and bioliquids, and the physical production of heating and cooling and electricity from biomass fuels has started. These criteria is applicable to following cases:

1. Installations for production of electricity, heating and cooling with a total rated thermal input equal to or exceeding 20 MW in the case of solid biomass fuels.
2. Installations for production of electricity in installations with a total rated thermal input below 50 MW.
3. Installations for production of electricity with a total rated thermal input from 50 to 100 MW applying high-efficiency cogeneration technology, or, for electricity-only installations, meeting an energy efficiency level associated with the best available techniques (BAT-AEELs) as defined in Commission Implementing Decision (EU) 2017/1442 [2].
4. Installations for production of electricity with a total rated thermal input above 100 MW applying high-efficiency cogeneration technology, or, for electricity-only installations, achieving a net-electrical efficiency of at least 36 %.

Calculation of the GHG emission reduction for the overall production of black pellets and for the co-firing of black pellets with pulverized coal shall be in accordance with the rules described in Annex VI of the European Directive 2018/2001, described in Section 2.5.

Energy efficiency

The Energy Efficiency Directive (EU) 2018/2002 [3] establishes an energy efficiency target of at least 32.5 % savings at European Union level by 2030. The EU Commission recommendation 2019/1659 [4] prioritizes the cost-effective use of waste heat from thermal power plants for district heating and cooling as a primary measure to contribute to the overall energy efficiency target in the European Union.

Sustainability of the feedstock

The supply of forest residues for production of black pellets shall fulfil the sustainability criteria defined in article 29 of the European Directive 2018/2001 [1].

Pellets quality requirements

Quality of wood pellets in accordance with European standard EN 14961-2 [5] or international standard ISO 17225-2 [6]. The standards include parameters and threshold values for dimensions (length and diameter), fines, mechanical durability, ash content, net calorific value as received and chemical composition.

Air emissions regulations

Co-firing of pellets shall fulfill Regulatory limits for emission of flue gas to air as shown in Table 4, in accordance with the European Directive 2010/75/EU [7] on industrial emissions.

This project has received funding from the European Union's Horizon 2020
research and innovation programme under grant agreement No 818349

Table 4: Limits for emissions to air (mg/Nm^3 at 6 % O$_2$ on dry basis) applicable to the PCC plant in compliance with Directive 2010/75/EU and connected regulations

Emission compound	**Set emission limit**
Carbon monoxide, CO	100
Nitrogen oxides, NOx	100
Total dust	5
Sulphur dioxide, SO$_2$	150
Hydrogen Chloride, HCl	8
Hydrogen Fluoride, HF	1
Cd + Tl	0.015

2.5 Value chain performance indicators

Energy production efficiency

Energy production efficiency is defined on an annual basis as the net energy produced, including the power and heat flow exported to the grid, divided by the total input energy along the value chain, which includes the energy of the coal and biomass feedstock at source and the energy consumption for harvesting and transporting the raw feedstock from the source to the PCC plant. The exported electricity and heat to the grid already account for consumptions both by the overall pretreatment and the PCC plant, and it is calculated from

$$\overline{\eta_e} = \int_0^T \left(\dot{W}_{el}^{EXP} + \dot{Q}_{th}^{EXP}\right) dt \;/\; \int_0^T \left[\left(\dot{H}_C^{SRC} + \dot{E}_C^{SRC} + \dot{E}_C^{TR}\right) + \textstyle\sum_i \left(\dot{H}_{B_i}^{SRC} + \dot{E}_{B_i}^{SRC} + \dot{E}_{B_i}^{TR}\right)\right] dt \qquad (1)$$

GHG emissions reduction

GHG emissions reduction is defined on annual basis as the net GHGs emissions generated along the whole value chain when replacing a fraction η_B of the total input energy to the PCC boiler with renewable energy. It is calculated based on the guidelines described in the European Directive 2018/2001 [1] from

$$\bar{r}_{GHG} = \left[(1-\eta_B)(m_{GHG,C}/\varepsilon_C) + \eta_B(m_{GHG,B}/\varepsilon_B)\right]/(m_{GHG,C}/\varepsilon_C) \qquad (2)$$

where $m_{GHG,C}$ and $m_{GHG,B}$ are the net mass of GHG emissions emitted along the value chain per unit energy of the input solid fuel, coal or SE pellets, into the boiler at the PCC plant, which are calculated respectively from $m_{GHG,B} = \sum_i \left(m_{GHG,B_i}^{EX} + m_{GHG,B_i}^{TR} + m_{GHG,B_i}^{PR} + m_{GHG,B_i}^{PPC}\right)$ and $m_{GHG,C} = \sum_i \left(m_{GHG,C}^{EX} + m_{GHG,C}^{TR} + m_{GHG,C}^{PPC}\right)$. In Eq. (2), the terms $\varepsilon_C = \varepsilon_{el,C}/\left[1 + (C_h/C_{el})\left(\varepsilon_{el,C}/\varepsilon_{h,C}\right)\right]$ and $\varepsilon_B = \varepsilon_{el,B}/\left[1 + (C_h/C_{el})\left(\varepsilon_{el,B}/\varepsilon_{h,B}\right)\right]$, where $\varepsilon_{el,K}$ and $\varepsilon_{h,K}$ represent the electricity and heat production efficiencies for coal and SE pellets, respectively, defined on annual basis relative to the fuel input based on its energy content.

Levelized cost of electricity

Levelized cost of electricity is defined as the average price per unit energy exported to the grid which is required so that the overall net present value (NPV) of the plant over its lifetime becomes zero. It is calculated from

$$C_{bf} = \sum_{i=1}^{N_B}\left[(1+r)^{-i}\left(C_{TPI_i}^{PCC} + C_{OP_i}^{PCC} - C_{COP_i}^{PCC}\right)\right] / \sum_{i=1}^{N}\left[(1+r)^{-i} t_{prod,i}\left(\dot{W}_{el}^{EG} p_{el} + \dot{Q}_{th}^{TG} p_{th}\right)\right] + \sum_{i=N_B}^{N}\left[(1+r)^{-i}\left(C_{TPI_i}^{PCC} + C_{TPI_i}^{PR} + C_{OP_i}^{PCC} + C_{OP_i}^{PR} - C_{COP_i}^{PCC} - C_{COP_i}^{PR}\right)\right] / \sum_{i=1}^{N}\left[(1+r)^{-i} t_{prod,i}\left(\dot{W}_{el}^{EG} + \dot{Q}_{th}^{TG} p_{th}\right)\right] \quad (3)$$

Here, r is the expected return of investment, $t_{prod,i}$ is the annual operating time, p_{th} is the market price for heat relative to the electricity, N_B is the period in years between the construction of the PCC plant to the construction of the retrofitting for co-firing biomass, N is the expected lifetime in years of the PCC plant, $C_{TPI_i}^{PCC}, C_{OP_i}^{PCC}, C_{COP_i}^{PCC}$ are the distribution of the annual total permanent investment, the operating costs and income from by-products for the PCC plant based on only coal from its construction to retrofitting, $C_{TPI_i}^{PR}, C_{OP_i}^{PR}, C_{COP_i}^{PR}$ are the distribution of the annual total permanent investment, the operating costs and income from by-products for the mechanical treatment and the steam explosion plant from its construction to the PCC plant lifetime, respectively.

3. Biomass availability and supply

3.1 Updated trends of forest wood availability up to 2050

The availability of forest wood is assumed to be dependent on the geographical location and annual timeframe. Estimations of the total demand for woody biomass to the total energy sector, including CHP production and biofuels production, and the current total use of the available forest wood for the EU28 and for individual European countries in the timeframe 2020-2050 are shown in Table 8. These results have been calculated based on the balance of the available forest wood for energy production (shown in Table 5), the total demand for woody biomass and waste to the European energy system (shown in Table 6) and the available waste for energy production (shown in Table 7). Projections of the total available waste for energy production consider the actual total annual production of renewable and non-renewable municipal solid waste (MSW), wood waste, organic vegetable and animal residues and industrial waste [8] extrapolated linearly up to 2050 based on the expected variations in population [9]. The available forest wood for energy production is estimated based on the net annual increase of available forest wood [10] and the demand for forest wood as material for industrial applications other than energy. Projections of the annual demand for wood by wood processing industry and 2030 and 2050 are estimated as proportional to the variation of the population for each country [9] based on the actual values obtained from Eurostat [11]. The total demand of biomass and waste to energy includes production of thermal power, district heating and biofuels for the transport sector based on the values reported by the EU regarding energy, transport and GHG emissions trends to 2050 [9]. In these estimations, the biomass and waste amount used for district heating are calculated from the total fuel input to district heating reported in [9] multiplied by a factor representing the official European targets of 20 % and 100 % share of renewable resources to district heating for 2020 and 2050. Table 9 shows the estimated share of the total forest area available for wood supply that is required to cover the total demand to the energy sector for individual European countries in the timeframe 2020-2050.

This project has received funding from the European Union's Horizon 2020
research and innovation programme under grant agreement No 818349

Table 5: Estimations of the distribution of availability of forest wood for energy between European countries in the timeframe 2020-2050

	Net amount of forest wood available (Mm³) [a]			**Industrial use of roundwood (Mm³) [b]**			**Forest wood available for energy (Mm³) [c]**			**Wood species (%) [d]**	
	2020	**2030**	**2050**	**2020**	**2030**	**2050**	**2020**	**2030**	**2050**	**SW**	**HW**
EU28	884.7	896.1	919.1	346.0	354.1	362.1	538.7	542.1	557.0	32.5	67.5
Austria	43.0	41.9	39.7	13.6	13.9	14.2	29.4	28.0	25.4	14.2	85.8
Belgium	6.0	5.8	5.5	4.2	4.3	4.4	1.8	1.5	1.1	35.9	64.1
Bulgaria	9.9	9.9	10.0	3.1	3.2	3.2	6.8	6.8	6.8	67.4	32.6
Croatia	8.3	8.2	7.8	3.5	3.6	3.7	4.8	4.6	4.1	81.1	18.9
Cyprus	0.0	0.0	0.0	0.0	0.0	0.0	0.0	0.0	0.0	8.1	91.9
Czechia	30.0	27.7	23.1	15.1	15.5	15.8	14.8	12.2	7.2	10.8	89.2
Denmark	4.6	4.9	5.4	1.6	1.7	1.7	3.0	3.2	3.7	26.1	73.9
Estonia	14.6	13.9	12.5	5.4	5.5	5.6	9.2	8.4	6.9	40.5	59.5
Finland	111.9	111.6	111.0	46.5	47.6	48.7	65.4	64.0	62.4	21.0	79.0
France	101.7	108.0	120.7	30.3	31.0	31.8	71.4	77.0	88.9	56.4	43.6
Germany	128.3	124.2	115.9	46.5	47.5	48.6	81.8	76.6	67.3	23.5	76.5
Greece	5.4	5.0	4.1	0.3	0.4	0.4	5.1	4.6	3.7	67.8	32.2
Hungary	12.9	12.6	12.1	2.8	2.9	2.9	10.1	9.8	9.2	87.1	12.9
Ireland	4.4	5.2	6.6	2.5	2.6	2.6	1.9	2.6	4.0	4.0	96.0
Italy	29.2	28.1	25.8	2.7	2.8	2.8	26.5	25.3	23.0	73.8	26.2
Latvia	20.2	24.7	33.5	10.5	10.7	11.0	9.8	13.9	22.5	38.3	61.7
Lithuania	12.3	13.4	15.7	5.3	5.4	5.5	7.0	8.0	10.2	46.4	53.6
Luxembourg	1.1	1.0	0.9	0.3	0.3	0.3	0.8	0.8	0.6	59.5	40.5
Malta	-	-	-	-	-	-	-	-	-	-	-
Netherlands	4.3	5.3	7.3	0.8	0.8	0.8	3.5	4.5	6.5	45.1	54.9
Poland	68.9	67.3	64.1	32.1	32.8	33.6	36.9	34.5	30.5	25.2	74.8
Portugal	18.3	18.0	17.2	9.3	9.5	9.7	9.1	8.5	7.5	60.0	40.0
Romania	36.7	36.1	34.9	10.8	11.1	11.3	25.9	25.1	23.6	61.9	38.1
Slovakia	12.5	12.9	13.8	9.3	9.5	9.7	3.2	3.4	4.0	33.5	66.5
Slovenia	9.4	9.1	8.5	1.9	1.9	2.0	7.5	7.2	6.5	46.1	53.9
Spain	30.5	29.8	28.4	11.2	11.5	11.8	19.3	18.3	16.6	65.8	34.2
Sweden	143.0	154.1	176.3	67.9	69.5	71.0	75.1	84.6	105.3	9.5	90.5
United Kingdom	17.3	17.6	18.2	8.5	8.7	8.9	8.7	8.9	9.3	4.9	95.1

Notes: [a] Available for wood supply from *[10]*; [b] Estimations for 2020 based on present values from *[11]*, Estimations for 2030 and 2050 as proportional to population based on *[9]*; [c] Calculated as the difference between net amount of forest wood and industrial use of wood; [d] Based on data from Eurostat *[11]* in 2017

Table 6: Estimations of the distribution of the total demand of biomass and waste to energy production (ktoe) between European countries in the timeframe 2020-2050

	Demand for biomass and waste to thermal power			**Demand for biomass and waste to district heating** [a]			**Demand for biomass and waste to biofuels** [b]		
	2020	**2030**	**2050**	**2020**	**2030**	**2050**	**2020**	**2030**	**2050**
EU28	54924	57152	77086	20813	19703	18478	26226	27228	29475
Austria	1627	1623	1890	757	738	600	586	595	716
Belgium	1799	1937	1715	78	28	72	739	785	920
Bulgaria	42	53	478	430	258	396	214	209	178
Croatia	28	33	68	0	0	0	71	62	64
Cyprus	1015	1219	1504	956	451	268	587	607	641
Czechia	13404	14128	16314	3556	2767	1923	3930	3883	4505
Denmark	1826	1560	2341	1204	1767	1451	356	350	431
Estonia	163	189	289	356	364	356	74	69	64
Finland	142	129	302	0	0	0	589	513	550
France	3024	2209	3778	0	0	0	2773	3290	3584
Germany	3725	3138	5744	1653	1639	1893	380	333	320
Greece	4524	5500	7041	828	941	581	3596	3828	4296
Hungary	28	163	246	118	119	125	180	166	152
Ireland	996	928	1469	368	417	358	396	419	458
Italy	219	378	533	0	0	0	402	419	480
Latvia	4545	5103	8790	96	117	32	2933	3146	3040
Lithuania	109	282	333	425	437	559	131	124	120
Luxembourg	84	100	94	1	1	0	213	228	266
Malta	219	220	548	410	444	422	95	84	91
Netherlands	8	11	19	0	0	0	16	15	15
Poland	2974	3168	3939	589	416	366	1027	995	1075
Portugal	2331	2951	4016	4277	5139	5514	1702	1790	1775
Romania	979	1371	2027	0	0	0	556	577	574
Slovakia	424	851	1269	595	399	185	492	451	412
Slovenia	5964	5136	6065	2475	1913	2351	561	579	668
Spain	161	147	286	83	72	31	190	193	208
Sweden	415	493	902	660	661	581	227	262	286
United Kingdom	4149	4132	5086	898	615	414	3210	3256	3586

Notes: [a] Calculated from the total fuel input to district heating reported in *[9]* multiplied by a factor representing the official European targets of 20% and 100% share of renewable resources to district heating for 2020 and 2050; [b] Assumed that total production of biofuels utilizes biomass and waste resources in Europe

Table 7: Estimations of the distribution of the potential available waste (four main fractions) to energy production (ktoe) between European countries in the timeframe 2020-2050

	MSW			**Wood waste**			**Animal and vegetal residues**			**Industrial waste**		
	2020	**2030**	**2050**	**2020**	**2030**	**2050**	**2020**	**2030**	**2050**	**2020**	**2030**	**2050**
EU28	34144	34967	34652	6988	7133	6983	2197	2581	2631	4056	4055	3929
Austria	608	641	675	0	14	27	0	13	26	463	474	485
Belgium	1788	1858	1961	304	331	371	15	99	225	289	304	326
Bulgaria	575	513	426	54	47	39	150	131	105	23	21	19
Croatia	131	149	166	2	2	2	3	6	8	2	2	2
Cyprus	688	688	678	6	6	4	20	20	19	244	244	242
Czechia	4866	4454	3125	2330	2243	1962	564	445	59	1297	1261	1146
Denmark	79	124	147	15	18	20	29	40	46	0	0	0
Estonia	97	97	85	57	57	49	0	0	0	0	0	0
Finland	1259	1273	1273	2	2	2	47	48	48	0	0	0
France	3386	3412	3447	26	39	56	36	57	85	0	0	0
Germany	479	494	494	907	924	924	43	49	49	48	49	49
Greece	5630	5990	6409	615	682	760	300	384	483	101	105	109
Hungary	376	386	376	2	2	2	6	10	6	12	12	12
Ireland	702	680	626	5	3	0	86	82	71	110	108	102
Italy	0	0	0	13	17	24	11	22	41	0	0	0
Latvia	4355	4571	4760	251	287	318	39	89	132	281	288	294
Lithuania	191	168	145	5	3	2	2	0	0	4	4	4
Luxembourg	53	53	71	11	11	13	0	0	6	14	14	16
Malta	105	93	70	3	3	3	17	14	8	3	3	3
Netherlands	76	76	76	3	3	3	3	3	3	0	0	0
Poland	1154	1212	1183	394	409	401	283	384	333	0	0	0
Portugal	839	767	491	409	387	304	33	17	0	531	520	477
Romania	1029	1043	1016	1	2	1	5	5	5	109	110	108
Slovakia	179	128	-3	492	460	380	42	35	17	90	87	79
Slovenia	13	77	155	596	625	661	31	65	106	18	19	20
Spain	118	131	118	26	28	26	3	6	3	51	53	51
Sweden	414	414	382	64	64	59	24	24	8	181	181	171
United Kingdom	4952	5474	6302	396	463	569	405	535	741	185	196	213

Notes: Projections of the total available waste for energy production consider the actual total annual production of renewable and non-renewable municipal solid waste (MSW), wood waste, organic vegetable and animal residues and industrial waste *[8]* extrapolated linearly up to 2050 based on the expected variations in population *[9]*

Table 8: Estimations of the distribution of the total demand of forest wood to energy based on the total demand of biomass and waste and the potential available waste to energy production (ktoe) between European countries in the timeframe 2020-2050

	Demand of biomass and waste to energy [a]			**Waste available for energy**			**Demand of forest wood to energy**		
	2020	**2030**	**2050**	**2020**	**2030**	**2050**	**2020**	**2030**	**2050**
EU28	85313	93575	125039	47385	48736	48195	64150	69033	96838
Austria	2364	2562	3206	1071	1142	1213	1293	1421	1993
Belgium	2554	2735	2707	2396	2591	2883	232	232	232
Bulgaria	342	382	1052	801	713	589	861	861	861
Croatia	232	385	523	138	158	179	558	558	558
Cyprus	99	95	132	958	958	943	2	2	2
Czechia	1793	2036	2413	9058	8404	6293	562	562	562
Denmark	2423	2735	4223	123	183	213	2300	2552	4010
Estonia	308	428	709	154	154	134	819	819	819
Finland	4436	4236	7957	1307	1322	1322	3128	2913	6635
France	8286	9767	11918	3448	3508	3588	4837	6259	8330
Germany	18045	19302	22742	1477	1515	1515	16568	17787	21227
Greece	731	642	852	6646	7161	7761	307	307	307
Hungary	1466	1542	2285	395	410	395	1070	1131	1890
Ireland	621	797	1013	903	873	799	73	73	73
Italy	7497	8304	11862	25	39	65	7473	8265	11797
Latvia	396	511	1061	4927	5235	5504	576	576	576
Lithuania	325	610	1012	202	175	150	542	542	862
Luxembourg	297	328	360	79	79	107	218	250	253
Malta	24	26	34	128	113	83	0	0	0
Netherlands	4119	4357	5380	82	82	82	4037	4275	5298
Poland	4888	7139	11305	1830	2005	1918	3058	5134	9387
Portugal	1535	1948	2601	1812	1691	1271	295	295	1330
Romania	1035	1488	1866	1145	1160	1130	1373	1373	1373
Slovakia	774	1063	1769	802	710	473	152	354	1296
Slovenia	368	374	525	657	786	942	279	279	279
Spain	5797	5499	7362	198	219	198	5599	5280	7164
Sweden	7020	6608	9084	683	683	620	6337	5925	8464
United Kingdom	7539	7675	9086	5939	6667	7825	1600	1008	1261

Notes: [a] Calculated as the sum of the total biomass and waste to thermal power production, a fraction of the total input fuel to district heating plants and the total input fuel to biofuels based on data from *[9]*

Table 9: Estimations of the distribution of the potential available forest wood to energy between European countries in the timeframe 2020-2050

	Available forest wood for energy production (Mm^3)			**Demand of forest wood to energy production (Mm^3)**		
	2020	**2030**	**2050**	**2020**	**2030**	**2050**
EU28	538.7	542.1	557.0	565.4	608.5	853.6
Austria	29.4	28.0	25.4	11.4	12.5	17.6
Belgium	1.8	1.5	1.1	2.0	2.0	2.0
Bulgaria	6.8	6.8	6.8	7.6	7.6	7.6
Croatia	4.8	4.6	4.1	4.9	4.9	4.9
Cyprus	0.0	0.0	0.0	0.0	0.0	0.0
Czechia	14.8	12.2	7.2	5.0	5.0	5.0
Denmark	3.0	3.2	3.7	20.3	22.5	35.3
Estonia	9.2	8.4	6.9	7.2	7.2	7.2
Finland	65.4	64.0	62.4	27.6	25.7	58.5
France	71.4	77.0	88.9	42.6	55.2	73.4
Germany	81.8	76.6	67.3	146.0	156.8	187.1
Greece	5.1	4.6	3.7	2.7	2.7	2.7
Hungary	10.1	9.8	9.2	9.4	10.0	16.7
Ireland	1.9	2.6	4.0	0.6	0.6	0.6
Italy	26.5	25.3	23.0	65.9	72.8	104.0
Latvia	9.8	13.9	22.5	5.1	5.1	5.1
Lithuania	7.0	8.0	10.2	4.8	4.8	7.6
Luxembourg	0.8	0.8	0.6	1.9	2.2	2.2
Malta	0.0	0.0	0.0	0.0	0.0	0.0
Netherlands	3.5	4.5	6.5	35.6	37.7	46.7
Poland	36.9	34.5	30.5	27.0	45.3	82.7
Portugal	9.1	8.5	7.5	2.6	2.6	11.7
Romania	25.9	25.1	23.6	12.1	12.1	12.1
Slovakia	3.2	3.4	4.0	1.3	3.1	11.4
Slovenia	7.5	7.2	6.5	2.5	2.5	2.5
Spain	19.3	18.3	16.6	49.3	46.5	63.1
Sweden	75.1	84.6	105.3	55.9	52.2	74.6
United Kingdom	8.7	8.9	9.3	14.1	8.9	11.1

3.2 Harvesting of forest wood

Harvesting of forest wood includes both the extraction of logs and the delivery of logs to the road. The annual cost, energy consumption and GHG emissions associated with the feedstock harvest, are calculated from

$$\begin{bmatrix} C^{EX}_{B_i} \\ E^{EX}_{B_i} \\ M^{EX}_{GHG,B_i} \end{bmatrix} = \dot{M}^{SRC}_{B_i} T_{prod} \left\{ \begin{bmatrix} c^{SRC}_{B_i,pr} \\ e^{SRC}_{B_i,pr} \\ m^{SRC}_{GHG,B_i,pr} \end{bmatrix} + \left(2\sqrt{\dot{M}^{SRC}_{B_i} T_{prod} / \pi f^{SRC}_{B_i} m_{S,B_i}} / 3 \right) \begin{bmatrix} c^{SRC}_{tr} \\ e^{SRC}_{tr} \\ m^{SRC}_{GHG,tr} \end{bmatrix} \right\} \quad (4)$$

where $\dot{M}_{B_i}^{F}$and T_{prod} represents the total input mass flow rate of raw woody biomass at source and the annual production time of the power plant, and $c_{B_i,pr}^{SRC}, e_{B_i,pr}^{SRC}, m_{GHG,B_i,pr}^{SRC}$ are the cost, energy consumption and GHG emissions per unit mass for production of logs at source. In Equation (4), m_{S,B_i} denotes the total mass of available wood per unit forest area, $f_{B_i}^{SRC}$ is the fraction of the total exploitable forest area which is available for procurement of wood to the specific value chain considered in this project and c_{tr}^{SRC}, e_{tr}^{SRC} and $m_{CO_2(eq),tr}^{SRC}$ are the cost, energy consumption and GHG emissions per unit mass per unit distance associated with the transport of logs inside the forest. The unit transport cost is here calculated as the sum of the distance-dependent and time-dependent costs, $c_{tr}^{SRC} = c_{L,tr}^{SRC} + c_{T,tr}^{SRC}/v_{avg}^{SRC}$, with v_{avg}^{SRC} representing the average transport speed in the forest.

3.3 Transport

Depending on the location of the forest relative to the PCC plant, the transport of feedstock can be road-based unimodal by truck or intermodal. Intermodal transport of the feedstock is here defined [12] as the transport of the same loading unit of feedstock that uses successively several modes of transport, including a combination of truck, train and shipping (without loading or unloading operations between modes). The annual cost, energy consumption and GHG emissions associated with the feedstock transport, are calculated from

$$\left[C_{B_i}^{TR}, E_{B_i}^{TR}, M_{GHG,B_i}^{TR}\right] = \dot{M}_{B_i}^{SRC} T_{prod} \left\{\sum\nolimits_{TM_i}\left[c_{B_i,tr}^{TM_i}, e_{B_i,tr}^{TM_i}, m_{GHG,B_i,tr}^{TM_i}\right]\right\} \tag{5}$$

where $c_{J,tr}^{TM_i}, e_{J,tr}^{TM_i}, m_{CO_2(eq),J,tr}^{TM_i}$ are the total cost, energy consumption and GHG emissions for transporting a unit mass of harvested wood to the power plant. Modelling of the transport cost for a generic transport mode $c_{J,tr}^{TM_i}$ considers the general approach most accepted in the literature [13] [14] for road-based unimodal and multimodal freight transport systems, which can be calculated from

$$c_{J,tr}^{TM_i} = c_{J,h}^{TM_i} + c_{J,ext}^{TM_i} + \left(c_{int,T}^{TM_i}/m_{j,tr_i}\right)\left(L_J^{TM_i}/v_{avg}^{TM_i}\right) + \left[1 + m_0^{TM_i}/\left(f_m^{TM_i} m_{tr}^{TM_i}\right)\right] c_{int,L}^{TM_i} L_J^{TM_i} \tag{6}$$

In this formulation, $c_{J,trf}^{TM_i}$, $c_{J,ext}^{TM_i}$, $c_{int,T}^{TM_i}$ and $c_{int,L}^{TM_i}$ denote, respectively, the cost for load handling, external cost and time-dependent and distance-dependent internal cost for each mode for transporting a unit mass. Distance-dependent internal transport cost includes fuel consumption, vehicle maintenance and tolls. Time-dependent internal cost includes labour, financial costs for the capital investment in the vehicle and depreciation of the load and the vehicle. Handling cost are associated with loading and unloading operations and transfer between transport modes. External costs represent indirect cost associated with impacts to human health, environment and wear of the transport network. The parameters $v_{avg}^{TM_i}$, $m_0^{TM_i}$, $m_{tr}^{TM_i}$and $f_m^{TM_i}$ in Eq. (7) represent the average speed, tare weight, the load factor and the load capacity of the specific transport vehicle used for each mode. The energy consumption and GHG emissions per unit transport mass are here calculated from

$$\left[e_{tr}^{TM_i}, m_{CO2(eq),tr}^{TM_i}\right] = \left[1 + m_0^{TM_i}/\left(f_m^{TM_i} m_{tr}^{TM_i}\right)\right] L_J^{TM_i} e_{L,tr}^{TM_i} \left[1, EF_{e,CO2(eq)}^{TM_i}\right] \tag{7}$$

where $e_{L,tr}^{TM_i}$ is the energy consumed per unit mass per unit distance and $EF_{e,CO2(eq)}^{TM_i}$is the GHG emission factor per unit energy consumed by the transport mode. Table 10 shows the reference values

This project has received funding from the European Union's Horizon 2020
research and innovation programme under grant agreement No 818349

considered for the parameters used in Eq. (5)-(7) to calculate the transport costs, energy consumption and GHG emissions.

Table 10: Parameters and values considered for evaluating the cost, energy consumption and GHG emissions associated with the transport of woody biomass in Europe

Transport mode	**Truck** [a]	**Train** [b] **(Electric / diesel)**	**Shipping** [c]
Tare weight (ton)	14.5	724	3800
Load capacity per shipment (ton)	21.8	2786	7200
Total weight (ton)	36.3	3510	11000
Load factor	0.85 [d]	0.75 [d]	0.75 [e]
Average transport speed (km/h)	60 [d]	65 [d]	30 [f]
Distance-dependent internal cost (Euro/t/km)	0.097 [f]	0.006 / 0.007 [f]	0.0018 [f]
Time dependent internal cost (Euro/h)	51.2 [g]	9.3 / 14.5 [g]	789 [g]
Handling internal cost (Euro/t)	4.14 [g]	5.7 [g]	1.5 [g]
External cost (euro/10^3 km)	18.5 [h]	4.5 / 14.8 [h]	16.5 [h]
Fuel consumption (l/km/10^3 ton)	22 [f]	- / 8.5 [f]	2.12 [j]
Net GHGs emissions (kg CO_2(eq.)/ton km)	0.087 [j]	0.04 [j]	0.011 [i]
Emission factors EF_i^f [k] CO_2 (kg / ton / km) C_nH_m (gr / ton / km) NO_x (gr / ton / km) SO_2 (gr / ton / km) PM (gr / ton / km)	 52.8 16.8 0.269 0 0.005	 7.9 2.5 0.003 0.001 0.005	 6.85 0.49 (CH4) 93.7 9.37 3.42

Notes: [a] Based on load capacity of 2 x 20ft containers; [b] It is assumed that a train consists of one locomotive of tare weight 100 ton and 26 flatcars of tare weight 24 ton and load capacity of 3 x 20ft containers [13]; [c] Based on tanker vessel Lo/Lo 11000 dwt; [d] From [13]; [e] Assumed as equal to train; [f] from [15]; [g] From [16]; [h] From [17]; [i] From [15] based on CO_2 emission factor for diesel; [j] From [18]; [k] Assumed distillate fuel oil as maritime fuel with emission factors from [19]

4. Production of black pellets via steam explosion

4.1 Overview

Steam explosion is defined [20] [21] [22] as a thermochemical treatment of biomass where the input particles are heated directly by pressurized saturated steam and then rapidly decompressed causing the fibrous structure of the biomass to break down. Steam explosion is currently considered a viable technological option for conversion of biomass feedstock to a solid energy carrier that can be compatible for direct co-firing in pulverized coal power plants [23]. The main reasons for this are:

1. The solid fraction has combustion properties (heating value and energy density) similar to coal.
2. The solid fraction has good binding properties, which facilitates pelleting.

This project has received funding from the European Union's Horizon 2020
research and innovation programme under grant agreement No 818349

3. Pellets produced from steam exploded biomass are durable, with low biological activity and low dust formation, with low risks for dust explosion, self-heating and ignition during storage and handling.
4. The solid product has lower alkali metals and chlorine concentrations compared to the input raw biomass, which can potentially reduce slagging and corrosion problems when co-firing.

4.2 Commercial status of steam explosion technology

The steam explosion technology for thermochemical treatment of wood was patented in 1926 by Mason [24] [25] using inlet steam temperature and pressure conditions of 285 °C and 35 bars with a residence time of the biomass particles of 2 minutes. Table 11 summarizes the current industrial implementation of the steam explosion technology. At present, the STEX technology has been demonstrated in industrially relevant environments by Arbaflame and Zilkha Biomass Energy (TRL 5-6). Based on proprietary ARBAKIT steam explosion technology, Arbaflame has been operating since 2003 an industrial scale demonstration plant for production of steam explosion pellets from sawdust derived from softwood (spruce and pine) in Grasmo (Norway) with a capacity of 6 ton/h and an accumulated production of 120,000 tons. The steam explosion pellets produced from the Grasmo plant have been tested in several coal-based power plants, including a full conversion from coal to ARBACORE in Ontario, Canada [22]. Zilkha Biomass Energy has been operating since 2015 a demonstration plant in Selma (Alabama, USA) for production of steam explosion pellets from sawdust and woodchips derived from forest residues with a capacity of 275,000 tons pellets per year. The process is highly reminiscent of the Arbacore process. The Finnish technology supplier Valmet has developed a pilot unit [26] implementing a proprietary technology (called BioTrac™) for the integration of steam explosion pellets and CHP production. In 2018, Valmet reached an agreement with the renewable energy company FICAP for the construction of a commercial steam explosion plant based on the BioTrac™ technology in France by 2020, with a combined annual capacity of 120 kton/year for black and white pellets [27]. It will be the first continuous steam explosion system at commercial scale.

Table 11: Producers of black pellets [28] [26] [27] [29]

Company	**ARBAFLAME**	**Zilkha**	**Valmet**	**FICAP** [a]
Location	Grasmo, Norway	Selma, Alabama, USA	Sundsvall, Sweden	Champagne-Ardenne, France
Commercial level	Commercial plant planned for 2020	Demonstration plant	Pilot unit	Commercial plant planned (2020)
Production capacity	6 ton/h (70 kton/year planned from 2020)	275 kton/year	n.a.	120 [b] kton/year (planned from 2020)
Dominant feedstock	Stem softwood (pine, spruce)	Sawdust, chips and forest residue (SW/HW)	Bark from softwood	n.a.

Notes: [a] Planned for 2020; [b] Includes both raw wood pellets and SE pellets

This project has received funding from the European Union's Horizon 2020 research and innovation programme under grant agreement No 818349

4.3 The steam explosion (SE) process

Operational parameters

The mass and energy yields, chemical composition and physical properties of the solid product from the steam explosion process depends on the following parameters:

- Chemical and physical properties of the input feedstock
- Steam temperature and pressure
- Residence time of the biomass particles
- Pressure release rate

Table 12 lists representative values for SE main operational parameters: (1) ranges used by the ARBAFLAME steam explosion process and (2) ranges from the literature [10] [17] [24] [25].

Table 12: Process variables for steam explosion of lignocellulosic biomass and for ARBAFLAME [10] [17] [24] [25]

Variable	**Unit**	**Literature ranges**	**ARBAKIT process**
Temperature	°C	190-240	215-222
Residence time	Minutes	4-10	8.3
Severity [a]	-	2-5	4.3-4.5
Pressure	Bar	10-41	24
Particle size	mm	0.1-12	<10
Moisture content	wt% wet basis	5-50	34

Notes: [a] See text below

Temperature and residence time are of vital importance for the total impact of the treatment. The severity factor in Table 12 is widely used for steam pre-treatment. It was developed by Overend et al. [30] assuming first-order kinetics and Arrhenius relation of temperature, and can be calculated from

$$S = log\left[\int_0^\tau \exp\left(\frac{T-100}{14.75}\right) dt\right] \tag{8}$$

where T represents the temperature in Celsius and τ is the residence time in s in the reactor. The severity factor is therefore linear in temperature and logarithmic in the residence time. The severity factor has been used successfully in the literature to correlate the main process performance parameters of the steam explosion process, such as the solid yield and the decomposition of the main constituents of the biomass [31] [30] [20]. Increasing the treatment severity has been shown to decrease the water uptake of the solid product, due to the removal of hydrophilic OH-groups [32]. Increasing the severity also leads to decreasing particle sizes of the SE biomass, as particle geometries shift from angular to more spherical shapes [32]. The pressure in the reactor has been shown to affect rate of degradation and the extent of xylose released from hemicellulose [33] [34], both increasing with pressure. The particle size of the input feedstock affects significantly both the heat transfer and the diffusion of steam into the particles. A too large particle size may lead to overheating and degradation on the surface and incomplete hydrolysis of the inner parts of the particles, due to heat

This project has received funding from the European Union's Horizon 2020
research and innovation programme under grant agreement No 818349

transfer limitations [35]. A smaller particle size increases the external surface to particle volume ratio and facilitate heat transfer, leading to increased rate of the thermochemical conversion and more homogeneous composition and properties of the solid product [32]. Moisture content of the input biomass does not seem to have a major direct effect on quality and yields of the steam exploded biomass [36] [32]. However, a higher moisture content will require more steam or other sources of heat for sufficient heating. Higher moisture content also slows down the heating rate, resulting in a lower (apparent) severity than for a dry sample [37] [25]. Steam to biomass ratio is another variable of interest. In order to properly heat and facilitate hydrolysis, sufficient amounts of steam is required, driving up the costs [35]. The higher the moisture content of the feedstock, the more steam is needed. Alternatively, additional heating from inert gases or an external heating jacket could supply parts of the heat required. The pressure release rate has little effect on the solid yield with sufficiently high temperature (above 240 °C) [27] in the steam explosion reactor, but affects the final particle size and degree of defibration [32] [34]; this is an important characteristic of the SE technology, activating the substrate and reducing the particle size further. The amount of oxygen in the reactor vessel can be adjusted in order to reduce the formation of hazardous gases. ARBAFLAME uses a partially oxidising atmosphere in the SE reactors. This adoption of a partially oxidising atmosphere, compared to a completely inert atmosphere, has been found to limit the formation of harmful VOCs as volatile organic compounds are oxidised, without the oxidisation of valuable non-volatile carbon. This oxidisation also supplies direct heating to the reactor's interior, reducing the heat demand from external sources. The oxygen concentration in the reactors used by ARBAFLAME are in the range 0.27-0.35 moles per kg dried biomass, which only corresponds to about 0.5 % of stoichiometric oxygen for complete combustion of the biomass [38]. The optimal conditions of the SE process varies significantly depending on the type of biomass (e.g. hardwood and softwood) and the particle size [39] [40]. For lignocellulosic biomass, the amount and structure of the three major components (cellulose, hemicellulose and lignin) affect the effectiveness of pre-treatment. Hemicellulose amount and composition also varies significantly between softwood and hardwood [41]. Softwood is regarded as a highly recalcitrant feedstock for SE pre-treatment, and a relatively high severity is required to produce a solid product with improved characteristics [42] [43] [20]. The majority of experimental investigations on the steam explosion of lignocellulosic biomass has been conducted under temperature and pressure conditions in the range 190-240 °C and 10-41 bar, with a residence time of 4-10 minutes. For the demonstration in the ARBAHEAT project, the ARBAKIT plant at Grasmo performs the SE treatment at around 220 °C and with a residence time of about 500 seconds, which combined corresponds to a relatively high severity. The SE process in ARBAHEAT uses feedstocks with a relatively high moisture content (approx. 34 % on wet basis), meaning less energy is used for pre-drying but more steam is needed in the SE reactor.

Solid yield, composition and properties

Table 13 displays key results from different studies on the effects of process parameters on solid yield, composition and properties of the solid product obtained from steam explosion of softwood and hardwood, and comparison with data from the analysis of ARBACORE pellets [32] [44] [23] [45]. In order to accentuate the effects of the process parameters and be able to compare across different feedstocks, the left column in each of three different feedstocks/products gives the absolute value, and the right column gives the percentage change compared to the feedstock after the treatment. The

This project has received funding from the European Union’s Horizon 2020
research and innovation programme under grant agreement No 818349

most notable effects of SE are (1) the increases in calorific value and carbon content due to oxygen depletion, and (2) significantly lower grinding energy requirement due to structural breakdown and increased brittleness [32]. The higher the severity, the higher the increase of both the calorific value and carbon content, particularly due to the degradation of oxygen-rich hemicellulose [34] [46] [47] [48] [49] [39]. In general, hardwood has a higher hemicellulose content, and the effectiveness of SE is usually higher. Sugars formed from hydrolysis of hemicellulose and depolymerised lignin can repolymerise into pseudo lignin [20] [50] [39] [51]. This, together with the degradation of hemicellulose, increases the apparent lignin content of the treated biomass. Lignin content and calorific value correlate positively, as lignin has a higher calorific value than cellulose and hemicellulose [52] [53]. Other fractions of the degraded hemicellulose may instead further degrade to volatiles following the steam fraction, resulting in lower solid yield. This degradation is higher as the severity increases [54]. Solid yields reported in the literature vary significantly, which can be due to variations in the other variables, besides severity, listed previously, but also feedstock or losses due to the experimental setup. Results from a handful of studies are shown in Figure 2. Another notable effect attributed to the degradation of hemicellulose is the hydrophobicity of the solid fraction after SE, which is increased with severity as this increases the extent of removal of OH-groups and the formation of pseudo lignin distributed evenly onto the material [25] [55]. The ash in SE material has been found to have a reduced alkali content [34] [55] [44]. The disruption of the cell structure and release of the soluble ash (e.g. alkali and alkali chlorides) which can be reduced by leaching. However, the concentration effect due to lost volatile matter will increase the relative ash content and thus works in the opposite direction, meaning that the ash content in the solid fraction not necessarily decreases [34]. Saeed et al., for example, found a higher ash content when examining the pine-based Zilkha Black Pellets, compared to untreated pine [56]. Hence, feedstock ash composition, treatment severity and possibly the amount of steam present can influence the ash concentration in the SE material. The volatiles produced from the degradation of hemicellulose, and some lignin and cellulose, include substantial amounts of VOC gases. Some of the emissions from the reactor can be mitigated using a partially oxidised atmosphere, however emissions continue during post-drying and storing. The composition of VOC is highly dependent on severity and feedstock. At mild severity, more terpenes with low boiling points are emitted, while more furans (e.g. furfural, hydroxymethylfurfural (HMF)) are emitted as severity increases [57]. The difference in composition between the pentose-based hemicellulose in hardwood and herbaceous plants and the hexose-based hemicellulose in softwood means furfural is expected to be more prominent using hardwood, while more HMF is expected from softwood.

This project has received funding from the European Union's Horizon 2020
research and innovation programme under grant agreement No 818349

Table 13: Fuel characteristics of softwood and hardwood for different severities, as well as the fuel characteristics of ARBACORE pellets. The softwood data is based on Lam [32], apart from the grinding energy which is from Wolbers et al. [23], and the hardwood on Biswas et al. [44]. ARBACORE data based on tests by ECN. Left column (each category): absolute values; right columns (each category): percentage compared to left column (200, for example, means a doubling of initial value)

	Softwood (Douglas fir)		**Hardwood (Salix)**		**ARBACORE**	
Severity	-	3.94/4.23/4.53	-	4.31/4.54/4.61	-	4.45
Temperature (°C)	-	200/220/220	-	220/228/220	-	220
Residence time (min)	-	10/5/10	-	6/6/12	-	8.3
HHV (MJ/kg dry basis)	18.82	101/103/105	19.88	107/110/109	20.24	105
Solid yield (wt% dry basis)	100	82/79/78	100	78/73/73	100	88-90
Energy yield (% HHV-based)	100	83/81/81	100	83/80/80	100	93-95
Fixed carbon (wt% dry basis)	14.3	123/145/156	16.4	109/118/114	16.22	120
Volatiles (wt% dry basis)	83.0	96/92/91	81.2	99/97/98	82.84	97
Ash (wt% dry basis)	2.7	71/81/65	2.4	83/83/75	0.94	32
C (wt% dry ash free basis)	48.44	104/108/110	50.6	106/108/108	50.28	104
H (wt% dry ash free basis)	6.23	98/96/95	6.25	100/100/100	6.08	102
O (wt% dry ash free basis)	45.28	95/91/90	42.8	94/92/92	43.34	96
N (wt% dry ash free basis)	0.22	n.a./82/77	0.30	114/134/117	0.24	42
S (wt% dry ash free basis)	n.a.	n.a.	0.044	88/88/93	0.06	17
Pelletizing energy (kWh/ton)	9.0	165/200/208	n.a.	n.a.	n.a.	n.a.
Grinding energy (kWh/ton)	29.2	23	n.a.	n.a.	n.a.	n.a.

Notes: Softwood ash content determined by TGA

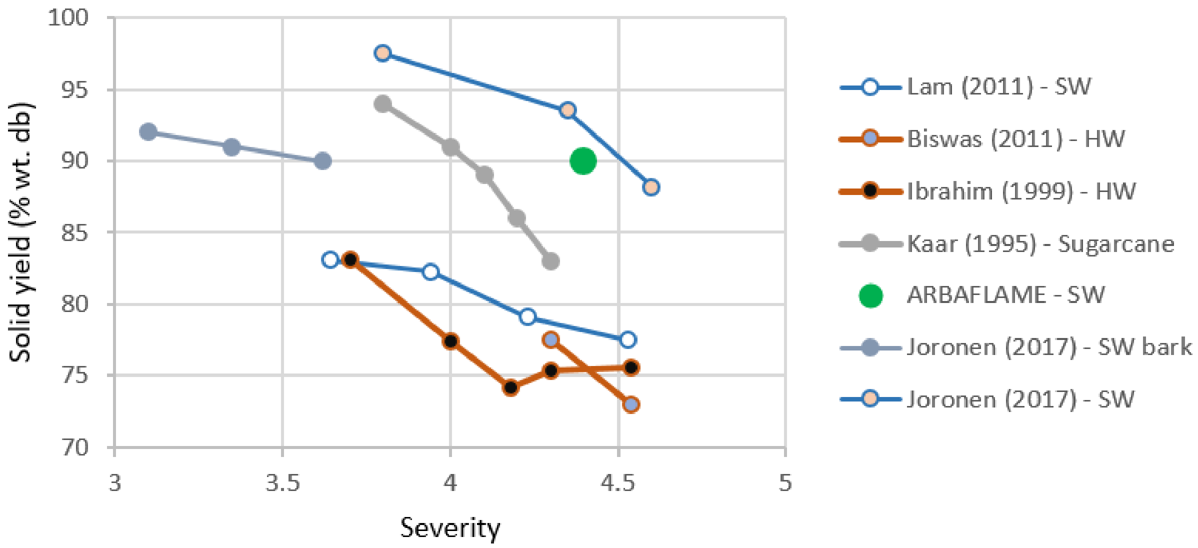

Figure 2: Solid yield as function of severity for a set of different studies using different feedstocks, Softwood (SW) has a blue colour, while hardwood (HW) is orange, ARBAFLAME operating severity and solid yield is also given (using SW). Data from Lam (2011) [32], Biswas (2011) [44], Ibrahim (1999) [49], Kaar (1995) [58], Joronen (2017) [25]

4.4 Pelleting of steam exploded biomass

Pellets from steam exploded biomass are durable, with low biological activity and low dust formation [32] [23]. This makes them suitable for storage and handling with low risks for dust explosion or self-heating and ignition. Pelleting is practically performed by either using a uniaxial piston-cylinder unit to produce single pellets or a pellet mill that consists of a series of rollers to compress raw material through a steel die [59]. Table 14 compares the main pelleting characteristics, measured experimentally [32] [60] [25] [23], of untreated and steam exploded woody biomass. Some studies suggest that SE wood (both hardwood and softwood) requires more energy to pelletize (about twice), increasing with treatment severity as shown in experimental data from Lam (2011) in Figure 3. Lam (2011) suggested that this additional energy could be attributed to the increased amount of extractives and mono-sugars which act as binders between particle surfaces and also stick to the die wall [32]. However, grinding energy is significantly reduced [23]. This can more than off-put the additional pelleting energy; it is also especially rewarding if the pelletizing step can be removed altogether, leaving only the reduced grinding energy and lower equipment and handling costs. In a humid environment, the equilibrium moisture content does not increase significantly for SE pellets, in contrast to white pellets, due to the hydrophobic nature of SE wood. While white pellets deteriorate completely when exposed to liquid water, the SE pellets can be stored outside in rain without any significant degradation or increase in moisture content [45] [23]. Volumetric energy density is 40-60 % higher in SE pellets compared to raw biomass pellets, lowering handling (especially transport) costs [23]. Durability of SE pellets is very high, while white pellets deteriorate faster during handling, creating high dust in the process. The quality of pellets produced from treated biomass is influenced by variables such as moisture content, temperature in the die, applied pressure, particle size and the number of binding agents in the biomass. Moisture acts as a binding agent and a lubricant in the pellet press, increasing the pellet quality and lowering the energy consumption in the pellet press. However, too high moisture content increases the viscosity [32] [61]; for wood a moisture content of around 10 % on wet basis is beneficial. Increasing the temperature of the die softens and activates the binders in the biomass, increasing the pellet quality. Increasing temperatures has also been shown to increase the density of the pellets. At 30 °C the natural binders in the biomass are not activated, and increasing temperature increases the pellet quality up to about 100 °C, after which some studies suggest a reduction in pellet quality and decrease of the density [62]. Increasing the pressure has a positive effect on both the density, hardness and durability of pellets, although the effect reaches a maximum beyond which an increase in pressure has little or no effect. For a given compacting pressure, increasing the treatment severity gives a higher pellet density [44] [32]. Van der Waals' forces, especially, depend on the particle size of the biomass as it increases with decreasing particle size [63]; the lower particle size due to both the thermal and mechanical breakdown from SE therefore increases the pellets quality [44]. The amount of natural binders in the biomass depends on the feedstock and the process conditions of the pre-treatment. Lignin is an important natural binder, and the higher the lignin content of the biomass, the higher the durability of the pellets appears to be [32].

This project has received funding from the European Union’s Horizon 2020
research and innovation programme under grant agreement No 818349

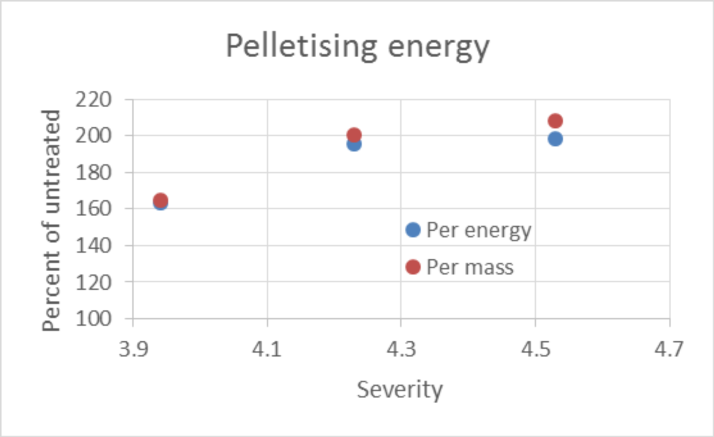

Figure 3: Plot of data from Lam. (2011). Pelleting energy per kg pellets and per unit fuel energy in percent of untreated wood

Table 14: Comparison of untreated and SE pellets [23] [13] [54]

	Bulk Density (kg/l)	**Energy density (GJ/m^3)**	**Durability**	**Milling equipment needs**	**Dust**	**Pelleting energy**	**Grinding energy**	**Hydrophobic**
Raw	0.55-0.65	8-11	Medium	Special	High	Medium	High	No
SE	0.70-0.80	13-15	High	Classic	Low	Higher	Low/coal-like	Yes

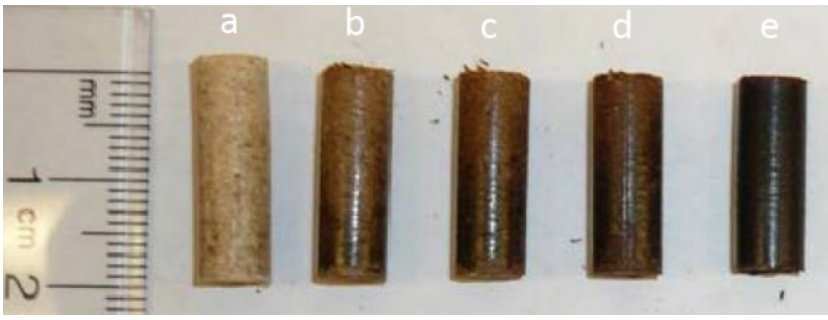

Figure 4: Pellets produced from SE softwood [32]. *From left to right: Untreated wood and increasing severity (from 3.6 to 4.5)*

4.5 Separation and valorisation of chemicals from the condensate produced from steam explosion of biomass

Chemical composition of the condensate from steam explosion of woody biomass

The steam explosion process produces an aqueous side-stream that contains a range of small organic molecules. The water phase generated when condensing the steam is of special interest, since it will contain most of the furfural produced by degradation of C_5 hemicellulose sugars during the steam explosion process. Furfural forms a low-boiling azeotrope with water, with a boiling point of around

This project has received funding from the European Union's Horizon 2020 research and innovation programme under grant agreement No 818349

96 °C [64]. The furfural will thus follow the steam in the steam explosion process. The condensed water will therefore contain considerable levels of furfural in addition to lower-boiling point (bp) organic by-products like methanol (bp 64.7 °), acetone (bp 56.05 °C), acetic acid (bp 118 °C) and formic acid (bp 100.8 °C). Most of the furfural produced in the steam explosion step is thus present in the aqueous condensate stream, as part of a quite simple mixture of organic compounds. Furfural has a limited solubility in water at 83 g/L, so the condensed vapour from azeotropic distillation will separate into a furfural bottom phase (density 1.16 g/ml), and an aqueous top phase. Further rectification of the furfural phase will produce pure furfural [65]. In addition, the residual moisture in the steam exploded material will retain higher-boiling products like HMF (hydroxymethylfurfural, a chemical of commercial interest) and dissolved sugars. Table 15 shows the chemical composition of a sample of condensed vapour produced from steam explosion of softwood (spruce and pine) at the Grasmo plant in Norway. These results show that furfural is the main chemical component, in agreement with previous experimental studies [66] [58]. Furfural is primarily formed from dehydration of hemicellulose and cellulose [55] [67]. The decomposition of hemicellulose and cellulose to monosaccharides and further conversion to furfural and HMF has been shown to increase with the severity of the SE treatment [68] [23] [58]. Kaar et al. [58] found the largest concentrations of furfural in the high severity and low temperature domain, with an exponential growth in the severity range 3.8-4.3. However, furfural is a reactive species and a further increase in severity will result in degradation and polymerisation of the produced furfural [69].

Table 15: Content of biobased chemicals in the condensate produced at Grasmo, Norway. Temperature and residence time: 215-217 °C and 500 seconds respectively

Compound	**Pine (vol%)**	**Spruce (vol%)**
Formic acid	0.10	0.06
Acetic acid	0.75	0.5
Acetone	0.09	0.05
Methanol	0.69	0.53
Furfural	1.30	0.92
Total sum	2.93	2.06

Chemicals market

Furfural is a versatile compound that allows for production of several value-added products [70]. The furfural market is expected to increase in volume and profit in the coming years, driven by the increasing demand for alternative – non-fossil – products as part of the transition to a green economy. The price of furfural is about 1 US$ per kg, but has been prone to quite large volatility in the last decades [70].

4.6 Mechanical treatment scenarios and characterization

As shown in Figure 5, the overall supply chain includes two scenarios for the mechanical treatment of biomass: 1) production of sawdust from logs through debarking and milling and sieving of wood logs for production of sawdust, and 2) chipping, grinding and sieving of wood logs and forest residues for production of microchips with particle size in the range of 5 to 10 mm.

This project has received funding from the European Union's Horizon 2020 research and innovation programme under grant agreement No 818349

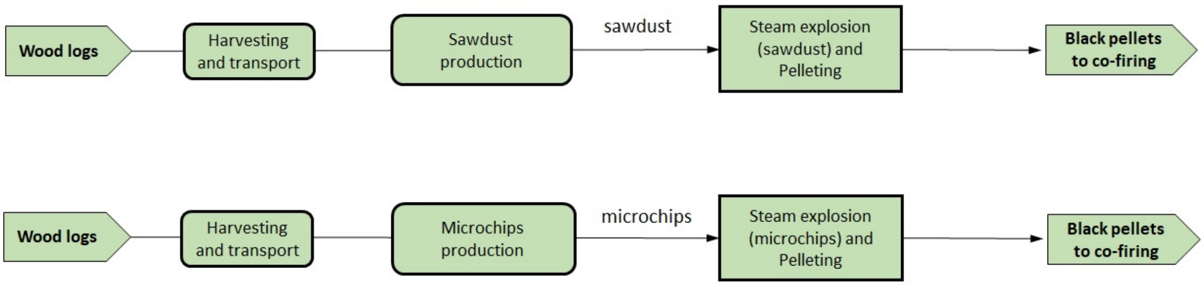

Figure 5: Schematic representation of the supply chain model for procurement of sawdust and microchips from wood logs to the steam explosion plant

Characterization of each mechanical treatment process MT_i is described in terms of the output particle size distribution $f^{MT_i}(d_p)$ and the total electric power consumed $\dot{W}_e^{MT_i}$which is calculated from $\dot{W}_e^{MT_i} = \dot{M}_S^{MT_i} w_e^{MT_i}$, where $\dot{M}_S^{MT_i}$ is the input feedstock mass flow rate and $w_e^{MT_i}$ is the specific electric energy consumed per unit input solid mass. Table 16 shows the literature data on the specific electric load for individual mechanical treatment processes.

Table 16: Specific electric load for mechanical treatment process of woody biomass

Process	**Power consumption (kWh/ton)**
Log debarking and milling (Beaver)	36.7
Logs chipping	6.9
Microchipping	42
Sieving	7
Hammer mill wood	11
Hammer mill SE wood	4

4.7 The ARBAFLAME steam explosion plant design and performance

Figure 6 shows the block diagram representing the process design of the steam explosion plant considered in the ARBAHEAT project, based on the ARBAKIT technology. The input biomass feedstock to the steam explosion plant considered is sawdust or microchips derived from wood logs. The overall conversion of input feedstock to black pellets include pre-drying of the raw biomass particles to reduce the moisture content to about 31 % on wet basis, steam explosion and flashing (pressure release) of the solid and vapour products and post-drying, pelleting and cooling of the solid product. Vapour streams from the flashing unit and the post-dryer are condensed using a water circuit that recovers the condensation heat to be used in the pre-dryer. Non-condensable gases from the steam explosion outlet vapour and the post-drying outlet vapour are combusted in a boiler with production of steam. The aqueous effluents from the condensers contain various chemicals and require further treatment before disposal. Table 17, Table 18, Table 19 and Table 20 show the main process design parameters, the mass and energy flows, and the electric loads for the ARBAFLAME steam explosion plant.

This project has received funding from the European Union's Horizon 2020 research and innovation programme under grant agreement No 818349

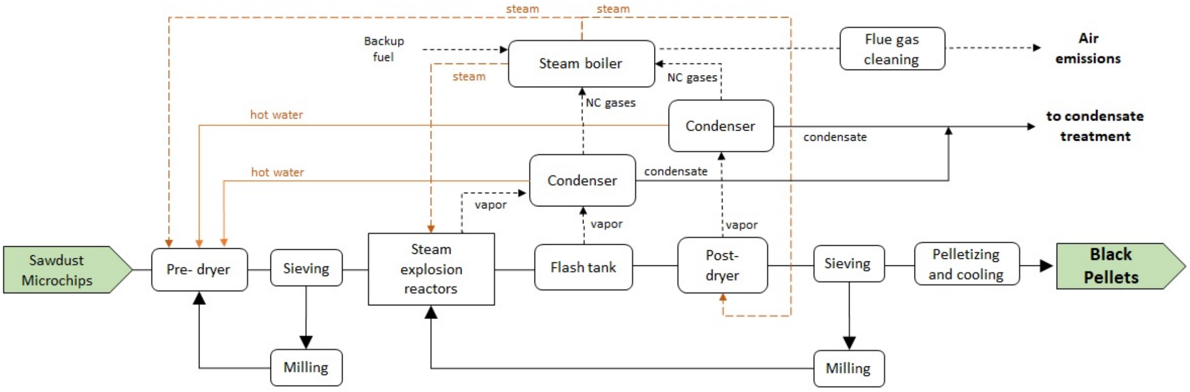

Figure 6: Schematic representation of the supply chain model for production of mechanically and thermochemically treated woody biomass for the PCC plant

Table 17: Process variables for steam explosion of lignocellulosic biomass for the ARBAKIT process [39] [32] [23] [71]

Variable	**ARBAKIT process**
Temperature (°C)	215-222
Residence time (min)	8.3
Severity (-)	4.3-4.5
Pressure (bar-g)	24
Particle size (mm)	<10
Moisture content (wt% wet basis)	34
Total heat duty pre-dryer (MJ/kg H_2O)	3.58
Process steam to SE reactor (kg/kg feed)	0.31
Heat duty post-dryer (MJ/kg H_2O)	2.67

Table 18: Mass flows for the ARBAKIT steam explosion plant based on sawdust as feedstock

Mass flows	**t/h**	**t/GJ (pellets)** [a]
Raw feedstock energy	6.7	0.38
Pre-dried feedstock	5.1	0.29
Solid product from SE	4.7	0.27
Pellets	3.2	0.18
Condensate from ARBAKIT	1.5	0.08
NC gases from ARBAKIT	0.6	0.03
Condensate from post dryer	1.3	0.07
NC gases from post dryer	4.3	0.24
Total condensate	2.8	0.16

Notes: [a] per unit chemical energy (GJ) of pellets produced from the SE plant

Table 19: Energy flows for the ARBAKIT steam explosion plant based on sawdust as feedstock

Energy flows	**MW**	**J/J (pellets)** [a]
Raw feedstock energy	16.2	0.92
Pre-dried feedstock	17.5	0.99
Solid product from SE	16.6	0.94
Solid product after post-dryer	17.6	1.00
Output pellets	17.6	1.00
Total condensate	0.6	0.03
Non-condensable gases	0.4	0.02
Net heat to pre-dryer	1.6	0.09
Heat recovered ARBAKIT condenser	0.7	0.04
Heat recovered post-dryer condensate	0.9	0.05
Steam to SE reactor	1.2	0.07
Heating jacket SE reactor	0.4	0.02
Net heat to post-dryer	1.0	0.06

Notes: [a] per unit chemical energy (J) of pellets produced from the SE plant

Table 20: Electric loads for the ARBAKIT steam explosion plant based on sawdust as feedstock

Electric load	**kWh/t** [a]
Dust receiving and scalping	1.5
Dust screening and sieving	4.0
Pre-drier	15.0
ARBAKIT unit	25.0
Post-drier	26.0
Pelleting	103.0
Milling dried wood	11
Mill SE wood	4

Notes: [a] per unit mass (ton) of input solid feedstock

This project has received funding from the European Union's Horizon 2020
research and innovation programme under grant agreement No 818349

4.8 Alternative pretreatment routes for co-firing into pulverized-coal power plants

Figure 7 shows a schematic representation of relevant routes (other than SE) for thermochemical treatment of woody biomass for production of solid fuel suitable for co-firing into pulverized-coal power plants.

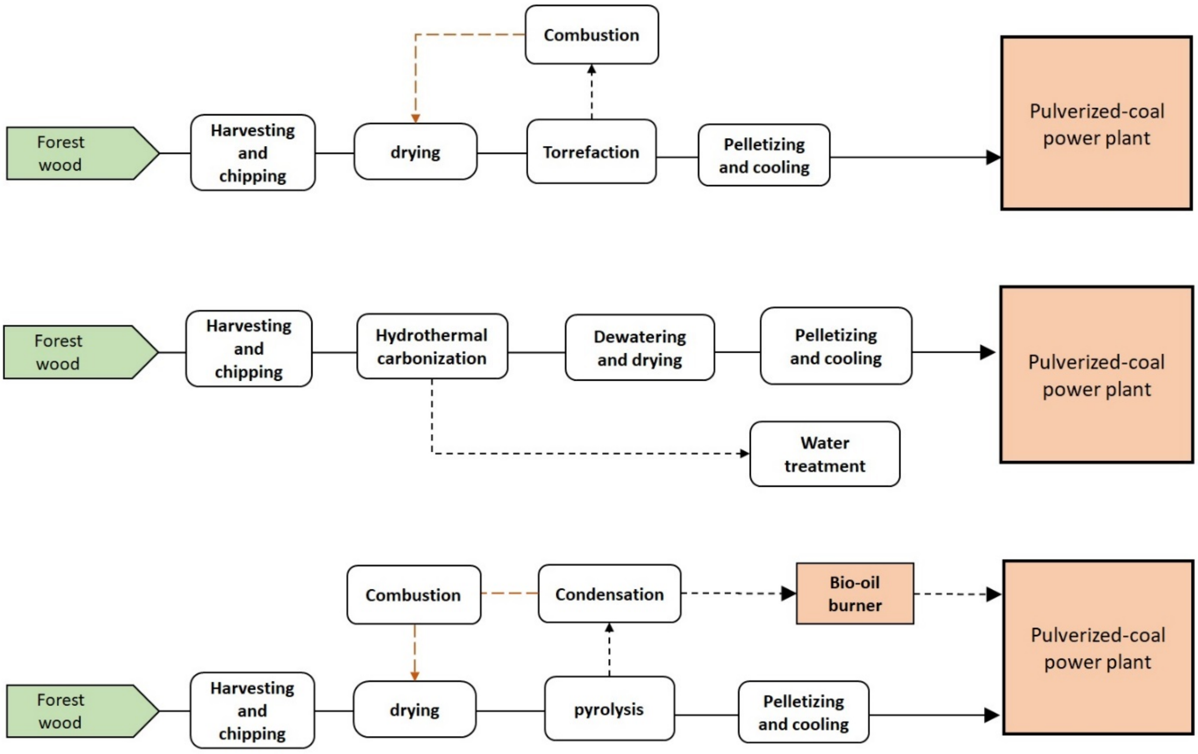

Figure 7: Schematic representation of alternative routes for pretreatment of woody biomass for co-firing into pulverized-coal power plant

Torrefaction

Torrefaction (TF) is a mild form of pyrolysis where the feedstock is heated to around 200-300 °C for 15-120 minutes at atmospheric pressure and in the absence of oxygen [72]. In these conditions the biomass is dried and partially decomposes, releasing volatiles (condensable and non-condensable). The least stable component hemicellulose is, just as during SE, degraded to the largest extent, releasing a flue gas with some combustibles which can be utilised to provide a fraction of the necessary process energy. TF, just like SE, partly destroys the OH-groups and makes the material hydrophobic, generally increasingly with treatment severity [66] [73]. Like the steam explosion process, torrefaction of woody biomass produces a substantial amount of VOC gases. Most of these gases is released during the process, but a small amount remains in the substrate and can be released slowly and cause a health risk (they have a distinct smell) [74]. The yields and product characteristics vary significantly between studies, especially depending on feedstock. In order to remove the variance due to feedstock and experimental setup and accentuate the influence key process parameters, Table 21 presents the data from one study only. The study is a comprehensive study by Tapasvi et al. on TF of relevant softwood

This project has received funding from the European Union's Horizon 2020 research and innovation programme under grant agreement No 818349

(Norway spruce) and hardwood (Norwegian birch) [73]. In this and other studies, it is evident that temperature is the most important parameter, ahead of residence time. The effect of particle size was also investigated, it had a smaller, but significant influence as well; increasing the particle size from 10 to 40 mm gave a solid yield increase by about 3 percentage points. The mass yield of the hardwood is generally lower for a given treatment severity, correlating with the higher hemicellulose content. The increase in heating value is also generally higher for hardwood. Ash content is increased by the concentration effect from mass loss [75]. The mass loss also leads to a substantial amount of energy loss. The volatile gas can be combusted, which increases the overall efficiency of the process [72]. The grinding energy required for size reduction of the TF material is significantly reduced compared to raw biomass. The reduction is higher for hardwood than softwood. This complies with other studies comparing grinding of TF material compared to untreated biomass, which show that grinding energy is reduced by 40-90 % compared to untreated wood and is highly dependent on process temperature [73] [76] [77] [72]. Agar et al. [78] found a decrease of 68-89 % in grinding energy after TF (250-300 °C), depending on feedstock, with a slightly higher decrease for hardwood than softwood. The moisture content of the torrefied substrate is too low (~2 %) to be ideal for pellet production, which is around 10-15 %, and additional water should be supplied to achieve high pellet quality and lower energy consumption [79] [80]. Using Norway spruce, pelleting energy was approximately 100 % higher than for raw sawdust, similar to that of SE [79].

Table 21: Feedstock characteristics of TF of softwood (Norway spruce) and hardwood (Norwegian birch). For each wood species, the left column is absolute value data of raw feedstock, and right column are the percent variation from the raw feedstock properties. The exception is yields and process parameters which are not stated for raw feedstock. Source: [73]

Wood species	**Softwood**			**Hardwood**		
Pressure (bar)	-	1		-	1	
Temperature (°C)	-	225	275	-	225	275
Residence time (min)	-	30/60	30/60	-	30/60	30/60
Solid product						
Mass yield (%) [b]	100	95/95	81/75	100	95/93	73/70
HHV (MJ/kg) [b]	20.45	101/101	106/108	19.80	101/101	107/108
Energy yield (%) [b]	100	95/95	86/81	100	96/94	75/73
Grinding energy (kWh/ton) [c]	161.4	52/44	34/25	171.9	41/41	23/19
VM (%) [b]	86.34	98/97	90/88	89.43	98/97	89/87
FC (%) [b]	13.43	147/152	207/233	10.35	117/128	191/213
Ash (%) [b]	0.23	105/100	182/91	0.22	105/177	114/182
C (%) [a]	50.10	104/105	112/114	48.62	102/103	110/112
H (%) [a]	6.36	97/97	92/90	6.34	97/94	89/89
O (%) [a]	43.52	96/95	88/86	44.90	98/98	90/89
N (%) [a]	0.07	111/78	78/100	0.09	111/111	133/133
S (%) [a]	0.05	100/100	100/100	0.05	100/100	100/100
Condensables						
Mass yield (%) [b]	-	4/4	15/20	-	4/5	22/23
Non-condensables						
Mass yield (%) [b]	-	1/1	4/5	-	1/2	5/7

Notes: [a] dry ash free; [b] dry basis; [c] percent of untreated

Hydrothermal carbonization

Hydrothermal carbonisation (HTC) is a pre-treatment where the feedstock is treated in compressed hot water (175-260 °C) at a pressure above the saturation point and a residence time from a few minutes up to 6 hours [81] [82] [80] [83]. Like SE and TF, HTC produces a solid fraction, called hydrochar, with many of the same characteristic improvements for use as a solid fuel. The overall efficiency of the HTC for production of solid fuel is less dependent on the moisture content of the feedstock, as the feedstock is suspended in the hot compressed water (HCW). After the treatment, the water can be removed mechanically, and thus more efficiently, from the solid product due to the morphological changes during treatment. HTC is therefore most often applied to feedstock with very high moisture content. The gas produced, roughly 10 % by mass, mainly consists of CO_2 and only small amounts of combustibles like CO [83] [80]. The liquid fraction contains solubilised sugars and degraded products, which could be utilised for production of valuable chemicals. Ash content is significantly reduced during HTC, as inorganic elements are dissolved in the liquid fraction [84] [80]. Table 22 outlines the changes in characteristics of biochar compared to raw softwood and hardwood for different temperatures and residence times from Bach et al. [80]. There is a significant difference between softwood (Norway spruce) and hardwood (Norwegian birch). The softwood had a solid yield of 8-20 percentage points higher than hardwood in the temperature range 175 to 225 °C, increasing with temperature. As with the other pre-treatments, this difference is usually attributed to the higher fraction of hemicellulose in hardwood, which has a higher degradation rate than the other biomass components. The increase in calorific value was roughly equal for both feedstocks, giving a roughly 10 percent points higher energy yield for softwood. While the HHV increase was limited to a maximum of 15 % in this study, other studies suggest that an increase of 30-40 % in HHV can be achieved using residence times of several hours, and suggest a more constant energy yield with temperature of around 75 % independently of mass loss [81]. Grindability is clearly shown to be highly dependent upon temperature and, to a lower degree, residence time, and is reduced by only 4-6 % compared to untreated wood when the process temperature is 225 °C. Pressure and particle size were shown to influence the solid yield, however to a lesser degree. A higher pressure reduced the solid yield with around 3 percentage points when using 160 bar compared to the saturation pressure of 15.5 bar (200 °C). Compared to 1 cm, a particle size of 3 cm increased solid yield by up to 5 percentage points for 10 minutes residence time and 220 °C. The effect was only 2-3 percentage points when increasing the residence time to 30 min. Using the MICUM test, Reza et al. compared the durability of TF pellets and HTC to a mix of the two [82]. The durability of TF pellets was found to decrease rapidly with temperature, from 77 % to 56 % from 250 to 300 °C, as more binding agents such as lignin are decomposed. HTC pellets (260 °C, 5 min) had a durability of 99.8 %. Larson et al. found a durability of 80-90 % for TF Norway spruce at 270-300 °C [79].

Table 22: Feedstock characteristics of HTC of softwood and hardwood wood species. For each wood species, the left column is absolute value data of raw feedstock, and right column are the percent variation from the raw feedstock properties. The exception is yields and process parameters which are not stated for raw feedstock. Source: [80]

Wood species	**Softwood**				**Hardwood**			
Pressure (bar)	-	70	70	70	-	70	70	70
Temperature (°C)	-	175	200	225	-	175	200	225
Residence time (min)	-	30	10/30/60	30	-	30	10/30/60	30
Water/Biomass (w/w)	-	5	5	5	-	5	5	5
Solid product								
Mass yield (%) ^{b}	-	88	83/79/74	70	-	80	67/65/64	58
HHV (MJ/kg) ^{b}	19.94	101	102/104/107	113	20.42	101	102/105/103	115
Energy yield (%) ^{b}	-	89	85/82/79	79	-	81	68/68/66	67
Grinding energy ^{c} (kWh/ton)	154	98	92/70/36	6	138	89	96/61/15	4
VM (%) ^{b}	86.50	99	98/97/95	86	89.46	99	98/95/92	82
FC (%) ^{b}	13.27	100	115/120/136	189	10.26	111	116/144/168	254
Ash (%) ^{b}	0.23	100	61/52/39	61	0.28	32	29/32/36	46
C (%) ^{a}	50.31	102	102/104/107	113	48.94	100	101/105/105	115
H (%) ^{a}	6.24	99	102/99/94	94	6.35	100	97/97/94	92
O (%) ^{a}	43.38	100	98/95/93	85	44.60	100	99/95/95	83
N (%) ^{a}	0.07	100	86/86/86	100	0.11	100	118/100/118	82

Notes: ^{a} dry ash free basis; ^{b} dry basis; ^{c} percent of untreated

Fast Pyrolysis

Fast pyrolysis (FP) is a pre-treatment technology where the feedstock is heated in an inert atmosphere at temperatures of 450-600 °C for typically less than 2 seconds, with production of biooil, char and non-condensable gases [85] [86]. The short residence time requires high heat transfer rates, requiring a particle size of no more than 3 mm [87]. Fast pyrolysis is optimized for achieving high yields of biooil, typically higher than 50 % and up to 80 % [88]; char yield is usually between 9-16 % and gas constitutes 13-28 % [86] [89]. The char produced has a much higher carbon content than the parent feedstock and a heating value similar to conventional coal. Biooil has a high oxygen and water content, giving a lower heating value comparable to or lower than the raw feedstock. Non-condensable gases from the pyrolysis process, containing mostly CO_2 and CO (> 90 % on mol basis) with smaller concentrations of hydrogen and light alkanes, are typically combusted to produce heat for the pyrolysis process [90]. Both the biooil and char from fast pyrolysis can be co-fired in pulverized coal power plants. Co-firing of bio-oil requires dedicated feeding system and burner. Table 23 outlines the analysis of fast pyrolysis oil and char produced from experiments in a fluidised bed reactor by Kim et al. [89] [91]. These works examined the effects of temperature and residence time on softwood and hardwood species with particle size around 0.5 mm. Biooil yield peaks around 500 °C and a residence time between 1-2 seconds, in line with other studies. At lower temperatures, lignin and anhydrosugars are not effectively released from the biomass matrix, while at higher temperatures the conversion to non-condensable gases becomes dominant [89]. Increasing the temperature reduces the char yield. Biooil yield is reduced with residence time above 2 seconds. The char yield increases with the residence time due to repolymerisation and recombination reactions taking place [89]. Biooil from softwood has a higher carbon content and calorific value than hardwood and a slightly higher energy yield. Earlier studies suggest that the ash content of the biomass in question is of significant importance to the oil and char yields [92]. When comparing a handful of fluidised bed experiments, Rogers et al. found that average organic oil yield would decrease from around 67 % to 50 % when the ash content in the feedstock increases from 0.5 % to 2.0 % [92]. Biochar from slow pyrolysis has significantly better grindability than raw biomass and the grinding energy can be reduced by as much as 90 % [93] [94]. However, there seems to be limited data available on the quantification of grindability of biochar from fast pyrolysis. Hu et al. [95] examined the pellet properties of wood pyrolysed for 30 min (slow pyrolysis). Pellets made from wood pyrolysed at 550-650 °C showed superior durability and density, but required also up to 50 % higher compression energy than wood pyrolysed at lower temperatures (250-450 °C). Ash content is significantly increased in biochar as most of the feedstock ash remains in the char [90]. Nitrogen content is slightly increased in biochar, while sulphur content is significantly reduced [90]. Chlorine content has been shown to be reduced during pyrolysis [96].

This project has received funding from the European Union's Horizon 2020
research and innovation programme under grant agreement No 818349

Table 23: Feedstock characteristics of pyrolysis oil and char from softwood and hardwood species. For each wood species, the left column is absolute value data of raw feedstock, and the right column is the percent variation from the raw feedstock properties. The exception is yields, process parameters and water content which are not stated for raw feedstock. Source: [89] [91]

Wood type	**Softwood**		**Hardwood**				
Species	Pitch pine/Japanese cedar		Oak/Eucalyptus		Yellow poplar		
Temperature (°C)	-	500	-	500	-	400/550	500
Residence time (s)	-	2.0	-	2.0	-	1.9	1.2/7.7
Oil							
Mass yield (%) [b]	-	61.6/62.6	-	65.7/59.2	-	50.2/63.9	68.3/51.6
Water (%) [c]	-	23.6/20.5	-	20.2/26.4	-	29.7/26.9	21.6/42.6
HHV (MJ/kg) [b]	17.9/19.2	102/98	17.8/16.5	96/94	17.9	84/94	96/58
Energy yield (%) [b]	-	63.0/61.6	-	62.7/55.6	-	42.3/60.3	65.6/30.0
VM (%) [b]	n.a.	n.a.	n.a.	n.a.	n.a.	n.a.	n.a.
FC (%) [b]	n.a.	n.a.	n.a.	n.a.	n.a.	n.a.	n.a.
Ash (%) [b]	0.5/0.4	n.a./n.a.	0.8/0.4	n.a./n.a.	0.58	n.a./n.a.	n.a./n.a.
C (%) [a]	46.8/48.8	94/103	45.7/46.4	91/83	48.8	73.7/83.0	85.2/58.2
H (%) [a]	6.0/6.1	110/110	6.0/5.9	118/115	6.5	100/93.8	92.3/129.2
O (%) [a]	47.1/45.1	104/95	48.3/47.6	106/115	44.5	128.5/119.1	117.3/141.6
Char							
Mass yield (%) [b]	-	16.5/13.9	-	14.1/14.9	-	29/9	9/18
HHV (MJ/kg) [b]	17.9/19.2	176/163	17.8/16.5	170/195	17.9	159.2/165.9	160.3/167.6
Energy yield (%) [b]	-	29.0/22.6	-	23.9/29.0	-	46.2/14.9	14.4/30.2
VM (%) [b]	n.a.	n.a.	n.a.	n.a.	n.a.	n.a.	n.a.
FC (%) [b]	n.a.	n.a.	n.a.	n.a.	n.a.	n.a.	n.a.
Ash (%) [b]	0.5/0.4	n.a./n.a.	0.8/0.4	n.a.	0.58	n.a./n.a.	n.a./n.a.
C (%) [a]	46.8/48.8	190/180	45.7/46.4	188/194	48.8	164.5/170.2	163.9/172.7
H (%) [a]	6.0/6.1	23/23	6.0/5.9	23/24	6.5	30.8/12.3	35.4/13.8
O (%) [a]	47.1/45.1	21/24	48.3/47.6	26/18	44.5	39.8/36.2	39.8/33.3
Gas							
Mass yield (%) [b]	-	21.9/23.5	-	20.2/25.9	-	21/28	23/30

Notes: [a] dry ash free basis; [b] wt% dry basis; [c] wt% wet basis

Comparison of pretreatment technologies

Table 24 lists process specifications for the different pre-treatment technologies, while Table 25 lists some feedstock characteristics and compares the composition of the different fuel alternatives. Table 26 lists pellet characteristics for the different pre-treatment technologies. However, different feedstocks cannot be compared directly to assess the suitability of each pre-treatment. HTC is well suited for wet biomass, such as seaweed and sewage sludge. SE show the most coal-like characteristics, especially considering the high solid and energy yield which can be upheld while improving characteristics. Other benefits for SE regarding combustion, emissions and ash deposits are discussed in section 5.3. TF is less advanced and requires less equipment but does not bring the solid fraction up to the same standard as the SE process. HTC increases the calorific value the most, however at the expense of high mass loss. Durability of pellets is better for SE and HTC, while TF wood disintegrate somewhat when exposed to mechanical stress. Grinding energy is reduces significantly for all treatment technologies.

Table 24: Process specifications for the different pre-treatment technologies

Process parameters	SE	TF	HTC	FP
Pressure (bar)	10-41	1	9-160 [a]	1
Temperature (°C)	180-240	200-300	175-250	400-600
Residence time (min)	4-12	10-120	5-360	<2 seconds
Particle size (mm)	2-12	<40	1-20	<3
Moisture content (wt% wet basis)	<55	<55	>70	<55
Oxygen feed (mol/kg dry basis)	0-0.35	0	0	0

Notes: [a] Above the saturation point for the corresponding temperature

Table 25: Feedstock characteristics of bituminous coal, average hard coal (TNO) and biomass. Source: [80] [97] [45]

Feedstock	Coal	Coal (TNO)	Untreated wood		Pretreated wood			
			SW	HW	SE ARBA	TF (SW/HW)	HTC (SW/HW)	FP (SW/HW)
VM [b]	27.85	29.01	86.34	89.43	80.2	78.13/79.98	74.74/73.78	n.a./n.a.
FC [b]	47.09	57.76	13.43	10.35	19.5	21.47/19.77	25.12/26.09	n.a./n.a.
Ash [b]	25.06	13.23	0.23	0.22	0.3	0.40/0.25	0.14/0.13	n.a./n.a.
C [a]	80.41	82.61	50.10	48.62	52.3	54.38/53.71	56.99/56.92	46.2/46.5 [c]
H [a]	5.30	4.83	6.36	6.34	6.2	5.81/5.65	5.87/5.86	6.0/6.0 [c]
O [a]	11.12	9.98	43.52	44.90	41.4	39.69/40.47	37.07/37.13	47.9/47.4 [c]
N [a]	1.69	1.81	0.07	0.09	0.1	0.07/0.12	0.07/0.09	n.a./n.a.
S [a]	1.48	0.77	0.05	0.05	0.01	0.05/0.05	n.a./n.a.	n.a./n.a.

Notes: [a] wt% dry ash free basis; [b] wt% dry basis; [c] average of two samples

Table 26: Pellet characteristics for different pre-treatment technologies

Process parameters	Coal	Untreated wood	SE	TF	HTC
Bulk Density (kg/l)	0.8-0.85	0.55-0.65	0.70-0.80	0.65-0.85	n.a. [a]
Energy density (GJ/m^3)	18-24	8-11	13-15	15-19	n.a. [a]
Hydrophobic	Yes	No	Yes	Yes	Yes
Durability	High	Medium	High	Medium / low	High
Milling	Classic	Special	Classic	Classic	Classic
Dust production	Low	High	Low	High	Low
Biological degradation	No	Yes	No	No	No

Notes: [a] Density and energy density for HTC pellets has been shown to be significantly higher than TF [82]

5. Co-firing of black pellets in a pulverized-coal power plant

5.1 Pulverized-coal combustion plant process design and performance

Figure 8 shows the process block diagram representing the pulverized-coal power plant at the Port of Rotterdam. The raw feedstock is stored outdoors and transported onsite by band conveyor. The solid fuel is milled, fed pneumatically and combusted in one single boiler. Combustion of the pulverized solid fuel is multi-stage with primary and secondary injection of the combustion air. The heat generated from combustion is recovered with production of steam at supercritical conditions. Flue gas cleaning includes catalytic reduction of NOx using ammonia as reducing agent, an electrostatic precipitator (for particles) and the removal of acid gases and remaining fly ash in a wet scrubber using lime. Table 27 shows the main operational parameters of the PCC plant. The nominal net electrical capacity is 731 MWe with a target availability of 93 % and a ramp up rate of 15-30 MW/minute. When running in base load mode, the power plant generates 5.5 TWh/year which represents a coal consumption of approximately 1.8 Mtons/year. Table 28 shows the average emissions to air.

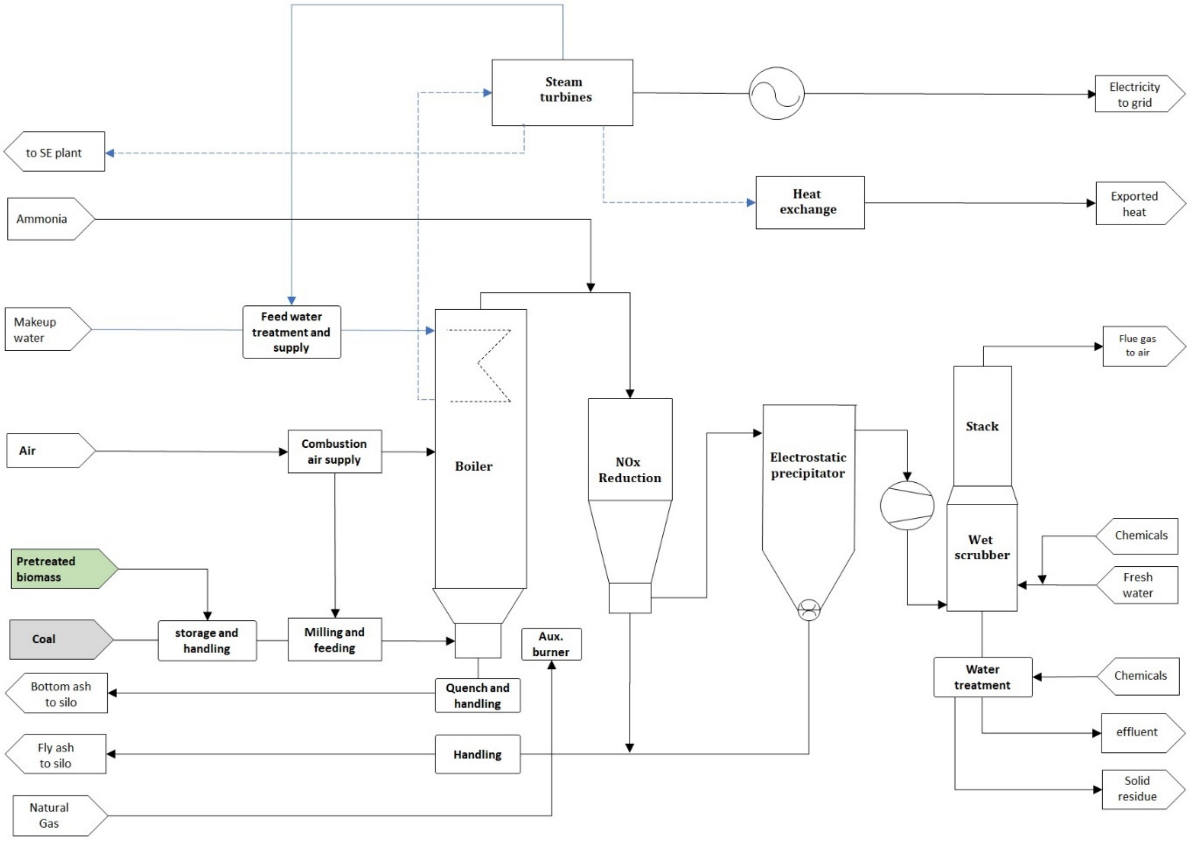

Figure 8: Process flow diagram for integration of the ARBAFLAME black pellets production plant into the ENGIE coal-based power plant

This project has received funding from the European Union's Horizon 2020 research and innovation programme under grant agreement No 818349

Table 27: Main process design parameters for the ENGIE pulverized-coal power plant at Port of Rotterdam

Variable	**Value**
Capital investment (MEuro)	1500
Input fuel power (based on LHV) (MW)	1673.3
Nominal electric power capacity (MW)	790
Net power output (MW)	730.1
Net power production efficiency (%)	43.63
Boiler efficiency (%)	93.95
District heating supply water temperature (°C)	70
District heating return water temperature (°C)	30
District heating thermal power (MW)	52.2
Internal power consumption (MW)	59.9
BM Water consumption (litre/ton input solid fuel) [a]	708.3
Tap water consumption (litre/ton input solid fuel) [a]	7.18
Ammonia (litre/ton input solid fuel) [e]	5.44
Limestone (kg/ton input solid fuel) [a]	34.74
Fuel oil (m^3/year)	2802
Electric power consumption (kWh/ton input solid fuel) [a]	225.4
Fly ash (kg/ton input solid fuel) [a]	115.45
Bottom ash (kg/ton input solid fuel) [a]	9.68
Gypsum (kg/ton input solid fuel) [a]	61.28
N-containing process water (litre/ton input solid fuel [a]	7.26
Drain sludge from scrubber (kg/ton input solid fuel) [a]	5.36

Notes: [a] per unit mass (ton) of input solid fuel into the PCC

Table 28: Emissions to air from the PCC plant based on hard coal combustion

Emission compound	**Emission to air**	**Set emission limit in compliance with Industrial Emissions Directive and connected regulations**
Carbon dioxide, CO_2 (g/kWh electricity generated)	690	-
Carbon monoxide, CO (mg/Nm^3) [a]	30	100
Nitrogen oxides, NOx (mg/Nm^3) [a]	41.2	100
Total dust (mg/Nm^3) [a]	1.5	5
Sulphur dioxide, SO_2 (mg/Nm^3) [a]	12.4	150
Hydrogen Chloride, HCl (mg/Nm^3) [a]	2	8
Hydrogen Fluoride, HF (mg/Nm^3) [a]	0.3	1
Cd + Tl (mg/Nm^3) [a]	0.0005	0.015

Notes: [a] 6 % O_2 on dry basis

5.2 Safety issues of storage and handling of black pellets

Dust explosion

Dust formation during handling of woody biomass and the consequent risk for dust explosion represents a major challenge when considering co-firing of biomass in pulverized-coal power plants [98]. Dust explosions are classified as primary and secondary [99]. Primary dust explosions occur within a contained dust volume, secondary explosions occur in dispersed dust layers accumulated on surfaces. The ignition sources leading to dust explosions are direct conductive heating or indirect radiative heating from hot surfaces or flames, self-ignition, or sparks generated by electric devices or by friction of two surfaces [99]. Explosion characteristics of biomass materials, defined and measured experimentally in accordance with standard methods [100] [101] [102] [103] [104] include:

Deflagration index, K_{st} represents the maximum rate of pressure rise for a deflagration in an ISO 1 m^3 explosion vessel when a dust is ignited. Powder material are classified based on the deflagration index as: non explosive $(K_{st} < 0)$, weak $(0 < K_{st} < 200)$, strong $(200 < K_{st} < 300)$ and very strong $(K_{st} > 300)$.

Maximum explosion pressure (P_{max}) is defined as the maximum over-pressure occurring in a closed vessel during the explosion of an explosive atmosphere determined under specified test.

Lower explosion limit (LEL) or minimum explosible concentration (MEC), defined as the lowest concentration of a combustible dust in mixture with air at which ignition occurs.

Minimum dust cloud ignition temperature (MDCT), defined as the minimum temperature that initiates a primary explosion within a dispersed volume of dust.

Minimum dust layer ignition temperature (MIT), defined as the minimum temperature that initiates a secondary explosion within a dust layer.

Table 29 summarizes the main explosion characteristics [105] [106] of different types of biomass materials and coal.

Table 29: Measured explosion characteristics of woody biomass materials and coal [105] [106]

	K_{st} **(bar m/s)**	P_{max} **(MPa)**	**MEC (g/m^3)**	**MIT (°C)**	**MDCT (°C)**
Coal	78	0.77	91		
Raw wood (spruce)	96-200	0.9-1	25-70	310	380
Southern pine	105	0.88	n.a.	n.a.	n.a.
Steam exploded wood	80	0.82	80	290	440
Wood pellets	98-146	0.77-0.84	n.a.	n.a.	n.a.
Torrefied spruce	110	0.91	54	n.a.	n.a.
Torrefied southern pine	115	0.77	55	n.a.	n.a.

This project has received funding from the European Union's Horizon 2020
research and innovation programme under grant agreement No 818349

Self-heating and self-ignition

Biomass materials undergo exothermic reactions, mainly by chemical oxidation or biologic degradation, which may generate sufficient quantities of heat to present a potential thermal hazard due to internal self-heating. Heat generation inside the bulk material is tempered by heat losses to the material's surrounding environment. For stockpiles, bins, silos, and other bulk containers, heat losses from the surfaces of the container must be considered together with proper mitigating measures.

5.3 Co-combustion of steam exploded pellets

Combustion of biomass has some challenges, including (1) non-homogenous fuel, (2) different combustion behaviour, (3) possibly impaired boiler efficiency compared to coal, (4) corrosion, (5) ash deposition [107] [97]. The pre-treatments discussed in this report increase the homogeneity of the biomass, increases the energy density and can reduce the amount of ash and alkali metals, all of which are limiting barriers to high co-firing ratio for raw biomass [108]. Direct co-firing where coal and fuel is mixed prior to handling requires significantly less retrofitting investments, but the fuel must have characteristics which do not cause impaired firing capabilities or problematic build-up of slag and/or corrosion [108]. Direct co-firing of raw biomass is common, with several hundred plants worldwide, but the co-firing ratios are usually less than 10 % (energy basis) [108] [97].

Thermal conversion efficiency

Variation in thermal conversion efficiency as a function of the co-firing factor can be calculated based on a simplified energy balance for the thermal conversion and the air pollution control as shown in Figure 9.

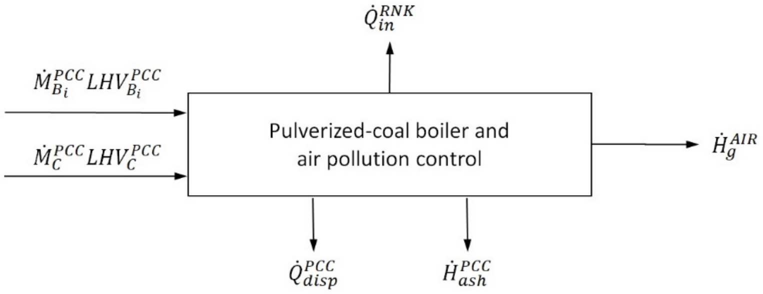

Figure 9: Schematic representation of the energy balance used for evaluating the thermal conversion efficiency when co-firing biomass and coal

The energy flows considered are the input energy in the pre-treated biomass and coal, denoted by $\dot{M}_{B_i}^{PCC} LHV_{B_i}^{PCC}$ and $\dot{M}_{C}^{PCC} LHV_{C}^{PCC}$respectively, the input thermal energy to the Rankine cycle $\dot{Q}_{in}^{RNK}$, the thermal enthalpy in the flue gas emitted to air $\dot{H}_g^{air}$, the thermal enthalpy of the ash $\dot{H}_{ash}^{PCC}$ and the dissipation heat loss through equipment and piping walls and cooling $\dot{Q}_{disp}^{PCC}$. In this work, it has been assumed that the input thermal energy to the Rankine cycle is constant and equal to the nominal design value for the plant running with coal only and that the heat loss due to dissipation and cooling is proportional to the input thermal energy to the Rankine cycle, $\dot{Q}_{disp}^{PCC} = f_{disp} \dot{Q}_{in}^{RNK}$. Assuming that the operational temperatures and heat transfer coefficients for dissipation and cooling through the thermal conversion and the flue gas cleaning systems are kept constant independently of the co-firing factor, the parameter f_{disp} can then also be assumed to be constant. The thermal enthalpy of the flue

This project has received funding from the European Union's Horizon 2020 research and innovation programme under grant agreement No 818349

gas and the ash can be written, respectively, as $\dot{H}_g^{air} = \sum_{B_i} \dot{M}_{B_i}^{PCC} h_{g,B_i}^{air} + \dot{M}_C^{PCC} h_{g,C}^{air}$ and $\dot{H}_{ash}^{PCC} = \dot{M}_{B_i}^{PCC} h_{ash,B_i}^{PCC} + \dot{M}_C^{PCC} h_{ash,C}^{PCC}$, where h_{g,B_i}^{air}, h_{ash,B_i}^{PCC} and $h_{g,C}^{air}$, $h_{ash,C}^{PCC}$ are the specific thermal enthalpy of the flue gas emitted to air and the ash produced from the thermal conversion of the pre-treated biomass and coal, respectively, calculated from $\left[h_g^K\right] = v_g^K\left(W_g^K/R\right) \cdot \left[c_{p,g}^K \cdot \left(T_g^{air} - T^0\right)\right]$ and $h_{ash,K}^{PCC} = y_a^K\left\{\left(f_{BA}^K y_{C,BA}^K + f_{FA}^K y_{C,FA}^K\right) \cdot h_C + (1 - y_{H2O}^K) y_a^K \left[f_{BA}^K c_{p,BA}^K (T_{BA} - 25) + f_{FA}^K c_{p,FA}^K \cdot (T_{FA} - 25)\right]\right\}$, where $K = B_i, C$ represent one specific input solid fuel into the boiler, $c_{p,BA}$ and $c_{p,FA}$ are the specific heat capacity of the bottom ash and fly ash, assumed to be 1.2 kJ/kg, $c_{p,g}^K$ is the specific heat of the flue gas emitted to air from conversion of an specific estimated from $c_{p,g}^K \sim c_{p,H_2O} \cdot X_{H_2O}^K + (1 - X_{H_2O}^K) \cdot \left[c_{p,N_2} + \left(c_{p,O_2} - c_{p,N_2}\right) \cdot X_{O_2}^K + \left(c_{p,CO_2} - c_{p,N_2}\right) \cdot X_{CO_2}^K\right]$ and v_{FG} is the normal volume of flue gas per unit mass of input solid fuel into the boiler, calculated from

$$v_g^K = R\,\{y_{H2O}^K + (1 - y_{H2O}^K)[y_C^K (W_{air}/W_C\,)(1 + x/4 - y/2)]\}/\left(W_g^K + X_{O2}^{air} \cdot W_{air}\right) \qquad (9)$$

with $x = (y_H^K W_C)/(y_C^K \cdot W_H)$ and $y = (y_O^K \cdot W_C)/(y_C^K \cdot W_O)$ denoting the H/C and O/C atomic ratios for the combustible fraction of the solid fuel transferred to the gas, R is the ideal gas constant and W_g^K representing the molecular weight of the flue gas produced emitted to air from the solid fuel K. In this notation, y and W denote mass fraction and atomic or molecular weight.

Here, T_{BA} and T_{FA} are the average temperature of the bottom ash leaving the boiler and the average temperature of the fly ash from the electrostatic precipitator, assumed to be 500°C and 300°C respectively, and T_g^{air} is the measured temperature of the flue gas emitted to air. From Figure 9, the thermal energy balance can be written as $\dot{M}_S^{PCC}\left(Y_C^{PCC} LHV_{B_i}^{PCC} + \sum_{B_i} Y_{B_i}^{PCC} LHV_{B_i}^{PCC}\right) = \dot{Q}_{th,out}\left(1 + f_{disp}\right) + \dot{M}_S^{PCC}\left[Y_C^{PCC}\left(h_{g,C}^{air} + h_{ash,C}\right) + \sum_{B_i} Y_{B_i}^{PCC}\left(h_{g,B_i}^{air} + h_{ash,B_i}\right)\right]$. Then, introducing the definition of thermal energy efficiency $\varepsilon_{th} = \dot{Q}_{th,out}/\left[\dot{M}_S^{PCC}\left(Y_C^{PCC} LHV_{B_i}^{PCC} + \sum_{B_i} Y_{B_i}^{PCC} LHV_{B_i}^{PCC}\right)\right]$ gives

$$\varepsilon_{th} = \left[(LHV_S^{PCC}/2)/(f_{disp} \cdot LHV_S^{PCC} + h_{ash} + h_g^{air})\right]\{-1 + 4\,(f_{disp} \cdot LHV_S^{PCC} + h_{ash} + h_g^{air})/LHV_S^{PCC}\}^{1/2} \qquad (12)$$

where $LHV_S^{PCC} = Y_C^{PCC} LHV_{B_i}^{PCC} + \sum_{B_i} Y_{B_i}^{PCC} LHV_{B_i}^{PCC}$ represent the net lower heating value of the solid fuel mix into the boiler.

Raw flue gas concentration

The total carbon content per energy unit is higher for biomass than for coal, increasing the gross CO_2 emissions per energy unit. Also, while there is usually some carbon left in the coal ash, the char burnout is almost 100 % for biomass, further increasing gross CO_2 slightly [97] [109]. Lower nitrogen and sulphur content in wood generally results in a significant reduction in fuel NOx and SOx emissions, as compared to coal [110] [111] [97]; the relative nitrogen and sulphur content in the fuel can thus be used to predict the relative fuel NOx and SOx emissions. However, emissions are highly dependent on the power plant and it might therefore be misleading to combine emissions from fuels not tested at the same plant. Differences in the possibility for reduced sulphur and nitrogen content in each of the pre-treatment technologies are not evident, and it is not straightforward to favour any, although ARBACORE shows significant improvements. Furthermore, the formation of NOx depends on other process conditions and the partitioning of nitrogen in volatiles and char, respectively. The effects of the different pre-treatment technologies on the behaviour of nitrogen upon devolatilisation and char formation must be known to accurately predict emissions [105]. When modelling the combustion of torrefied biomass, Li et al. found that the fuel NOx almost linearly decreases with co-firing ratio [97]. They also found that the ratio of air NOx to fuel NOx (roughly 0.5) was roughly constant, giving a linear decrease in the total NOx emissions [97]. The nitrogen content of the TF biomass used was 0.5 wt%, compared to 1.27 wt% for coal, and the NOx emissions were modelled to be reduced by half (52 %) when 100 % of coal was replaced. Lower chlorine content generally reduces the potential HCl emissions [112]. Chlorine content in biomass can be higher or lower than coal, and the pre-treatment technologies ability to reduce this can therefore be of significant importance [112]. As mentioned, the amount of chlorine in the pre-treated biomass can potentially be reduced for all three methods (through leaching and/or volatilisation), although it is not clear that the volatile loss during TF outweigh the relative mass loss. Woody biomass has a low content of trace elements, significantly lower than coal for most, and these elements are not seen as problematic regarding ash or air emissions.

Ash slagging and fouling

Both untreated and thermochemically treated woody biomass have significantly lower ash content than coal. However, the chemical composition of the ash from biomass depends greatly on the biomass species, local soil [85] and pre-treatment conditions and has a higher complexity than that of coal. Differences in the chemical composition and mineralogy structure of the ash can lead to lower melting temperatures depending mainly on temperature and oxidizing or reducing local conditions inside the boiler, possibly enhancing slagging and fouling [113]. Experimental investigations on the ash behaviour in biomass combustion [114] [115] [116] [117] [118] have shown that higher concentrations of alkali metals (K, Na), alkaline earth metals (Ca, Mg) and silicon lead to an increase of slagging and fouling, while higher concentrations of Cl lead to increase of corrosion on heat exchanger surfaces. The removal of alkali and earth alkali elements through leaching can reduce the potential risks of problematic ash deposition. Leaching can also reduce the content of corrosive elements like chlorine, depending on the form at which it is present in the feedstock (e.g. leachable salts, associated with organic matter, etc.). The analysis of SE ARBACORE pellets, performed by TNO in delivery D1.2, showed much lower content of ash-forming elements than a representative choice of raw feedstocks. Total ash content was reduced by around 70 %, and also a 90 % or more reduction in chlorine. For HTC the ash content is significantly reduced due to the leaching effect of wet chemistry. During TF, the concentration effect is driving an increase in ash content, and limited ash is removed during the process.

The analysis of ARBACORE pellets highlights significant reduction in virtually all problematic components for ash deposition, corrosion and emissions, generally better than what is found in literature, both for SE and the other pre-treatment technologies. However, the other pre-treatment options also show mostly improved characteristics, if not as significant as ARBACORE.

This project has received funding from the European Union's Horizon 2020
research and innovation programme under grant agreement No 818349

6. Preliminary analysis of the value chain

This section reports a preliminary evaluation of the overall performance of the value chain, based on the following main assumptions

1. The feedstock basis for co-firing into the PCC plant include hard coal and ARBACORE pellets according to the characterization shown in Table 30.
2. The SE pellets production plant, including mechanical pretreatment, is assumed to be integrated into the PCC plant.
3. Coal is supplied from one source located at constant distance from the PCC plant.
4. The raw biomass feedstock is assumed to be wood logs harvested from forest. The source of wood logs is assumed to be distributed around the PPC with a surface area dependent on the annual mass flow of logs required. Logs are transported to the PCC plant by truck.
5. Production of black pellets is performed by steam explosion of both sawdust and microchips. The overall process performance of the SE plant as well as the chemical composition and physical properties of the SE pellets using microchips and sawdust as feedstock is assumed to be the same. More detailed analysis considering differences in the process, equipment design and costs when using sawdust or microchips will be undertaken later in the project as part of the scale-up analysis and costing in task 5.4 of WP5.

6.1 Material and energy flows

Table 31 and Table 32 show preliminary calculations of the main material and energy flows along the value chain for the co-firing of pellets produced from steam explosion of woody biomass in the PCC plant of Rotterdam.

6.2 GHG emissions balance

Table 33 and Table 34 shows preliminary calculations of the main GHG emissions along the value chain as a function of the co-firing ratio of black pellets into the PCC plant, based on respectively microchips and sawdust. Figure 10 compares the variation with the co-firing ratio of the GHG emissions per unit energy of pellets along the overall production of SE pellets from logs based on mechanical treatment of logs to microchips and sawdust. Figure 10 compares the variation of the co-firing ratio of the overall GHG emissions reduction along the value chain.

6.3 Cost analysis

Table 35 and Table 36 shows estimations of the total capital investment for the installation of the SE pellets production plant and retrofitting of the PCC plant as a function of the co-firing ratio, based on respectively microchips and sawdust. Table 37 shows estimations of the operating cost for production of SE pellets and co-firing of SE pellets and coal into the PCC plant. Figure 11 compares the variation of the co-firing ratio of the overall production cost per unit energy of black pellets (left) and net exported electricity from the PCC plant (right).

This project has received funding from the European Union's Horizon 2020 research and innovation programme under grant agreement No 818349

Table 30: Characterization of the hard coal and SE pellets considered in the preliminary analysis of the value chain

Feedstock	**Hard coal**	**ARBACORE**
Moisture (wt% wet basis)	8.88	3.9
Volatiles (wt% dry basis)	29.01	82.6
Fixed Carbon (wt% dry basis)	57.76	17.2
Ash (wt% dry basis)	13.23	0.2
HHV (MJ/kg dry basis)	25.82	21.3
C (wt% dry ash free basis)	71.68	53.2
H (wt% dry ash free basis)	4.19	6.2
O (wt% dry ash free basis)	21.86	40.49
N (wt% dry ash free basis)	1.57	0.1
S (wt% dry ash free basis)	0.67	0.01
Cl (wt% dry ash free basis)	0.033	0.003

Table 31: Main mass flows for co-firing of SE pellets into the PCC plant in Rotterdam

Co-firing factor		**0**	**0.25**	**0.5**	**0.75**	**1**
Coal consumption	ton/h	233.3	175.0	116.7	58.3	0.0
Wood logs	ton/h	0.0	164.5	329.0	493.4	657.9
Sawdust	ton/h	0.0	148.0	296.1	444.1	592.1
Pellets consumption	ton/h	0.0	70.7	141.4	212.1	282.8
Combustion air	Nm^3/h	3078.4	3133.0	3187.7	3242.3	3296.9
Flue gas	ton/h	2166.8	2223.7	2280.6	2337.5	2394.3
Cooling water [a]	m^3/h	171.0	171.0	171.0	171.0	171.0
Fresh water	m^3/h	1.68	1.76	1.85	1.94	2.03
Fly ash	ton/h	25.95	19.59	13.23	6.86	0.50
Bottom ash	ton/h	2.18	1.64	1.11	0.58	0.04
Gypsum	ton/h	14.30	15.06	15.81	16.57	17.33
Ammonia	m^3/h	1.27	1.34	1.40	1.47	1.54
Limestone	ton/h	8.10	6.12	4.14	2.16	0.18
Fuel oil (aux. burner)	$m^3/year$	2802.0	2802.0	2802.0	2802.0	2802.0
Process water	m^3/h	1.69	1.78	1.87	1.96	2.05

Notes: [a] Used by the condenser of the Rankine cycle

This project has received funding from the European Union's Horizon 2020 research and innovation programme under grant agreement No 818349

Table 32: Main annual energy flows (GWh/year) for co-firing of SE pellets into the PCC plant in Rotterdam

Co-firing factor	**0**	**0.25**	**0.5**	**0.75**	**1**
Coal to PCC boiler	13051.7	9788.8	6525.9	3262.9	0
Fuel to coal mining and washing	490.9	368.2	245.4	122.7	0
Fuel to coal transport	257.6	193.2	128.8	64.4	0
Wood logs to SE pellets prod.	0.0	3586.9	7173.9	10760.8	14347.8
Pellets to PCC boiler	0.0	3262.9	6525.9	9788.8	13051.7
Fuel to wood logs harvesting	0.0	134.8	269.7	404.5	539.4
Fuel to wood logs transport	0.0	37.6	86.8	143.4	206.1
Heat to SE plant	0.0	412.3	824.6	1236.9	1649.2
Fuel oil to PCC aux. burner	34.8	34.8	34.8	34.8	34.8
Ash residue from PCC plant	79.0	59.6	40.3	20.9	1.5
Dissipation heat PCC plant	261.0	261.0	261.0	261.0	261.0
Flue gas from PCC plant	456.1	468.1	480.1	492.1	504.0
Net electricity exported to grid	5694.78	5516.82	5338.86	5160.90	4982.94

Table 33: Main GHG emissions (ton CO_2-eq) per unit energy (GJ) of the input solid fuel to the boiler of the PCC plant in Rotterdam as a function of the co-firing factor based on microchips as input to the Steam Explosion

Co-firing factor	**0**	**0.25**	**0.5**	**0.75**	**1**
Coal supply	**16.4**	**12.3**	**8.2**	**4.1**	**0.0**
Exploitation	10.7	8.1	5.4	2.7	0.0
Transport	5.6	4.2	2.8	1.4	0.0
Black pellet supply from microchips	**0.0**	**22.0**	**44.5**	**67.5**	**90.7**
Log harvest	0.0	2.9	5.9	8.8	11.8
Log transport	0.0	2.0	4.6	7.5	10.8
Microchipping. SE and pelleting	0.0	17.0	34.1	51.1	68.1
Net Flue gas [a]	**333.9**	**250.4**	**167.0**	**83.5**	**0.0**
Fuel oil combustion	**0.6**	**0.6**	**0.6**	**0.6**	**0.6**
Ash disposal	**0.73**	**0.55**	**0.37**	**0.19**	**0.01**
Total GHG flows (microchips to SE)	**351.6**	**285.8**	**220.6**	**155.8**	**91.4**

Notes: [a] Only contribution from coal combustion

This project has received funding from the European Union's Horizon 2020
research and innovation programme under grant agreement No 818349

Table 34: Main GHG emissions (ton CO_2-eq) per unit energy (GJ) of the input solid fuel to the boiler of the PCC plant in Rotterdam as a function of the co-firing factor based on sawdust as input to the Steam Explosion

Co-firing factor	**0**	**0.25**	**0.5**	**0.75**	**1**
Coal supply	**16.4**	**12.3**	**8.2**	**4.1**	**0.0**
Exploitation	10.7	8.1	5.4	2.7	0.0
Transport	5.6	4.2	2.8	1.4	0.0
Black pellet supply from sawdust	**0.0**	**22.5**	**45.7**	**69.2**	**93.1**
Log harvest	0.0	2.9	5.9	8.8	11.8
Log transport	0.0	2.0	4.6	7.5	10.8
Sawdust prod. SE and pelleting	0.0	17.6	35.2	52.9	70.5
Net Flue gas [a]	**333.9**	**250.4**	**167.0**	**83.5**	**0.0**
Fuel oil combustion	**0.6**	**0.6**	**0.6**	**0.6**	**0.6**
Ash disposal	**0.73**	**0.55**	**0.37**	**0.19**	**0.01**
Total GHG flows (sawdust to SE)	**351.6**	**286.4**	**221.8**	**157.6**	**93.7**

Notes: [a] Only contribution from coal combustion

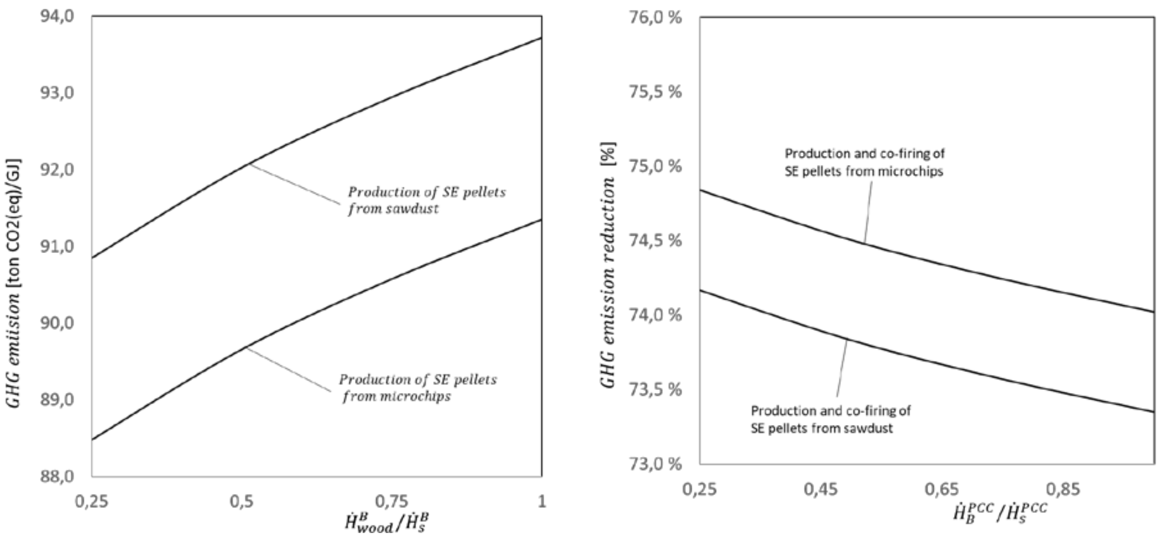

Figure 10: Net GHG emissions per unit pellets energy for the overall production of black pellets from steam explosion of woody biomass as sawdust and microchips

This project has received funding from the European Union's Horizon 2020 research and innovation programme under grant agreement No 818349

Table 35: Capital investment cost (MEuro) for the development and construction of the steam explosion production plant based on microchips and retrofitting of the PCC plant as a function of the co-firing factor

Co-firing factor	**0**	**0.25**	**0.5**	**0.75**	**1**
Equipment cost SE pellets production	**0.00**	**59.22**	**94.47**	**124.33**	**151.17**
Microchipping	0.00	6.33	9.93	12.93	15.59
Pre-dryer	0.00	2.76	4.18	5.34	6.34
SE system	0.00	21.60	35.95	48.43	59.83
Post-dryer	0.00	5.41	8.19	10.45	12.42
Pelletizer	0.00	7.49	12.17	16.16	19.77
Process water treatment	0.00	7.54	12.25	16.27	19.90
Silos and conveyors	0.00	4.46	6.01	7.15	8.09
Electrical system	0.00	0.72	1.15	1.51	1.83
Instrumentation & control system	0.00	2.91	4.63	6.09	7.39
Project costs SE pellets production	**0.00**	**39.09**	**62.35**	**82.05**	**99.77**
Land and site preparation	0.00	11.84	18.89	24.87	30.23
Foundation and buildings	0.00	4.44	7.09	9.32	11.34
Plant engineering	0.00	5.03	8.03	10.57	12.85
Contingency	0.00	10.36	16.53	21.76	26.45
Project development and licenses	0.00	1.48	2.36	3.11	3.78
Commissioning	0.00	5.92	9.45	12.43	15.12
PCC plant retrofitting cost	**0.00**	**3.03**	**5.00**	**6.73**	**8.31**
Mills modifications	0.00	0.19	0.38	0.57	0.76
Bunker modifications	0.00	0.02	0.03	0.05	0.06
Steam supply to SE plant	0.00	0.95	1.54	2.05	2.51
Combustion system condensate	0.00	0.98	1.59	2.12	2.59
Combustion system NC gases	0.00	0.49	0.79	1.05	1.29
Civil work	0.00	0.27	0.44	0.59	0.73
Electrical system	0.00	0.13	0.22	0.30	0.37
Total Investment cost	**0.00**	**101.33**	**161.82**	**213.11**	**259.24**

Table 36: Capital investment cost (MEuro) for the development and construction of the steam explosion production plant based on sawdust and retrofitting of the PCC plant as a function of the co-firing factor

Co-firing factor	**0**	**0.25**	**0.5**	**0.75**	**1**
Equipment cost SE pellets production	**0.00**	**65.04**	**103.60**	**136.22**	**165.50**
Debarking and milling	0.00	12.15	19.07	24.82	29.92
Pre-dryer	0.00	2.76	4.18	5.34	6.34
SE system	0.00	21.60	35.95	48.43	59.83
Post-dryer	0.00	5.41	8.19	10.45	12.42
Pelletizer	0.00	7.49	12.17	16.16	19.77
Process water treatment	0.00	7.54	12.25	16.27	19.90
Silos and conveyors	0.00	4.46	6.01	7.15	8.09
Electrical system	0.00	0.72	1.15	1.51	1.83
Instrumentation & control system	0.00	2.91	4.63	6.09	7.39
Project costs SE pellets production	**0.00**	**42.93**	**68.38**	**89.90**	**109.23**
Land and site preparation	0.00	13.01	20.72	27.24	33.10
Foundation and buildings	0.00	4.88	7.77	10.22	12.41
Plant engineering	0.00	5.53	8.81	11.58	14.07
Contingency	0.00	11.38	18.13	23.84	28.96
Project development and licenses	0.00	1.63	2.59	3.41	4.14
Commissioning	0.00	6.50	10.36	13.62	16.55
PCC plant retrofitting cost	**0.00**	**3.03**	**5.00**	**6.73**	**8.31**
Mills modifications	0.00	0.19	0.38	0.57	0.76
Bunker modifications	0.00	0.02	0.03	0.05	0.06
Steam supply to SE plant	0.00	0.95	1.54	2.05	2.51
Combustion system condensate	0.00	0.98	1.59	2.12	2.59
Combustion system NC gases	0.00	0.49	0.79	1.05	1.29
Civil work	0.00	0.27	0.44	0.59	0.73
Electrical system	0.00	0.13	0.22	0.30	0.37
Total Investment cost	**0.00**	**111.00**	**176.99**	**232.85**	**283.04**

This project has received funding from the European Union's Horizon 2020
research and innovation programme under grant agreement No 818349

Table 37: Annual operating cost (MEuro/year) for production of SE pellets and the PCC plant as a function of the co-firing factor

Co-firing factor	**0**	**0.25**	**0.5**	**0.75**	**1**
Coal procurement	**148.8**	**107.5**	**71.6**	**35.8**	**0**
Wood logs harvest and transport	**0**	**65.2**	**142**	**226.3**	**316.6**
SE plant labour	**0**	**0.73**	**0.82**	**0.93**	**1**
SE plant maintenance cost	**0**	**1.35**	**2.16**	**2.83**	**3.44**
SE plant insurance and taxes	**0**	**0.68**	**1.08**	**1.42**	**1.72**
PCC plant operational labours	**3.78**	**3.78**	**3.78**	**3.78**	**3.78**
PCC plant consumables & utilities	**5.60**	**5.39**	**4.57**	**3.74**	**2.92**
Limestone	2.206	2.04	1.38	0.72	0.06
Ammonia	0.589	0.55	0.39	0.22	0.06
Fuel oil aux. burners	2.802	2.802	2.802	2.802	2.802
PCC plant residues and effluents	**0.49**	**0.62**	**0.65**	**0.68**	**0.71**
Fly ash	0.446	0.4	0.27	0.14	0.01
Bottom ash	0.064	0.057	0.038	0.02	0.001
Gypsum	-0.77	-0.63	-0.49	-0.35	-0.21
Effluents	0.75	0.79	0.83	0.87	0.91
PCC plant stack emissions	**43.58**	**32.69**	**21.79**	**10.9**	**0**
PCC plant operational services	**0.35**	**0.35**	**0.35**	**0.35**	**0.35**
PCC plant port activities	**0.19**	**0.19**	**0.19**	**0.19**	**0.19**
PCC plant maintenance labour	**3.18**	**3.18**	**3.18**	**3.18**	**3.18**
Maintenance Services and travelling	**0.16**	**0.16**	**0.16**	**0.16**	**0.16**
Depreciation	**23.05**	**23.05**	**23.05**	**23.05**	**23.05**
Annual operational cost	**229.2**	**244.9**	**275.4**	**313.3**	**357.1**

This project has received funding from the European Union’s Horizon 2020 research and innovation programme under grant agreement No 818349

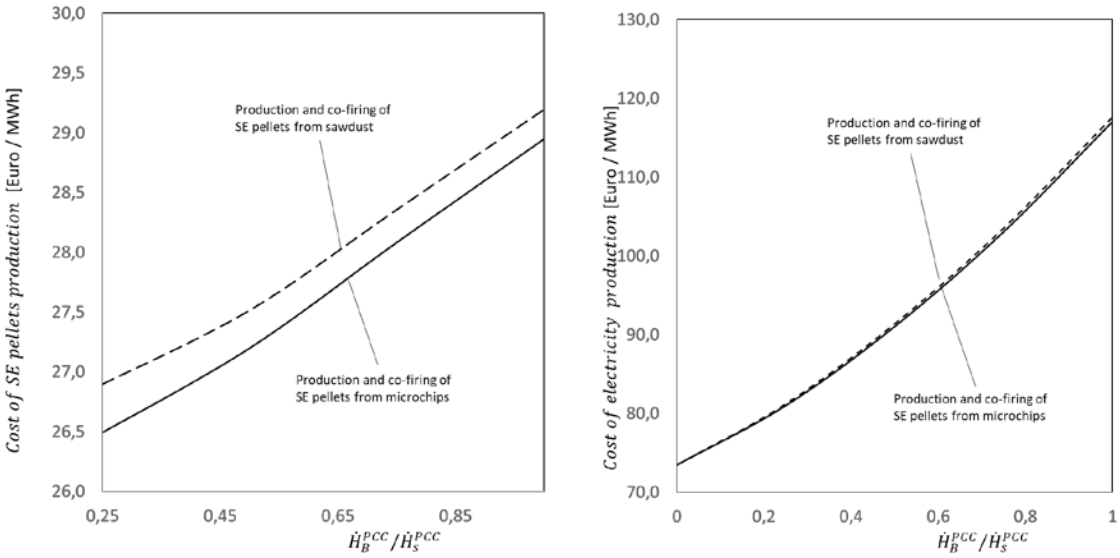

Figure 11: Cost of SE pellets production (left) and cost of electricity production (right) as a function of the co-firing ratio based on steam explosion of microchips (solid line) and sawdust (dashed line)

7. Conclusions

The state-of-the-art production of black pellets from steam explosion of woody biomass and co-firing into a pulverized-coal power plant has been reviewed. The overall approach has been to establish a reference value chain framework where the main aspects and parameters related to the process, environmental and economic performance have been evaluated based on the state-of-the-art.

Since pulverized-coal power plants typically operate at large scale, co-firing of black pellets requires procurement of woody biomass from multiple sources located both locally and across Europe. In this scenario, the energy consumption, GHG emissions and cost along the supply chain of the biomass feedstock to the PCC plant become significant and highly dependent on the availability of the forest wood. The availability of forest wood across Europe and within the timeframe 2020-2050 has been evaluated considering the potential forest area available for wood supply, the demand of wood resources to the wood processing industry and the overall energy sector, and the availability of other biomass and various waste resources. This analysis has shown that the availability of forest wood for CHP production is expected to decrease significantly due to the high demand for production of biofuels.

Steam explosion of woody biomass with production of black pellets has been shown to be a suitable thermochemical treatment technology for co-firing of biomass into pulverized-coal power pants. The steam explosion process exhibits high mass and energy yields, with increased heating values and energy densities compared to the input biomass. The solid product is highly hydrophobic and brittle, and exhibit milling properties compatible with coal. The solid yield has good binding properties, which facilitates pelleting. Pellets produced from steam exploded biomass are durable, with low biological activity and low dust formation, with low risks for dust explosion, self-heating and ignition during storage and handling. The solid product has lower alkali metals concentrations compared to the input raw biomass, which can potentially limit slagging and corrosion problems when co-firing.

Considering alternative thermochemical processes for converting woody biomass to black pellets suitable for co-firing in pulverized-coal combustion plant, i.e. Torrefaction (TF) and Hydrothermal Carbonization (HTC) and fast pyrolysis (FP), the steam explosion process shows the most coal-like characteristics and higher solid and energy yields. Pellets produced from TF of woody biomass exhibits low durability and high production of dust, which is an important shortcoming in commercial co-firing applications due to dust explosion issues. HTC of woody biomass can achieve the highest calorific values among the SE and TF, however at the expense of high mass loss. One main advantage of the HTC process is the ability to reduce inorganics from the feedstock due to the leaching properties of water, which leads to better ash slagging and fouling problems during combustion.

Preliminary estimations of the process and economic performance of the value chain show that co-firing SE pellets in large-scale PCC plan can achieve 74.8 and 73.5 reduction of the GHG emissions for co-firing ratios between 25 and 100 %, respectively. The reduction of GHG emissions is slightly higher when considering production of black pellets from microchips rather than sawdust due to the lower electricity required for mechanical pretreatment. On the other hand, increasing values of the co-firing ratio leads to higher cost of electricity, which can reach above 120 Euro / MWh for 100 % co-firing ratio, mainly due to high harvest and transport supply cost of woody biomass and the additional investment cost in the biomass pretreatment.

References

[1] “Directive (EU) 2018/2001 of the European Parliament and of the Council of 11 December 2018 on the promotion of the use of energy from renewable”.

[2] “Commission Implementing Decision (EU) 2017/1442 of 31 July 2017 establishing best available techniques (BAT) conclusions, under Directive 2010/75/EU of the European Parliament and of the Council, for large combustion plants”.

[3] “Directive (EU) 2018/2002 of the European Parliament and of the Council of 11 December 2018 amending Directive 2012/27/EU on energy efficiency”.

[4] “Commission Recommendation (EU) 2019/1659 of 25 September 2019 on the content of the comprehensive assessment of the potential for efficient heating and cooling under Article 14 of Directive 2012/27/EU”.

[5] “EN 14961-2, Solid biofuels – Fuel specification and classes – Part 2: Wood pellets for non-industrial use,” 2012.

This project has received funding from the European Union’s Horizon 2020
research and innovation programme under grant agreement No 818349

[6] "ISO 17225-2, Solid biofuels - Fuel specifications and classes - Part 2: graded wood pellets," 2014.

[7] "Directive 2010/75/EU of the European Parliament and of the Council of 24 November 2010 on industrial emissions (integrated pollution prevention and control)".

[8] "European Bioenergy Outlook 2019: Biomass Supply," 2019.

[9] "EU Energy, transport and GHG emissions: trends to 2050. Reference scenario 2013".

[10] "Forest biomass for energy in the EU: current trends, carbon balance and sustainable potential for BirdLife Europe, EEB, and Transport & Environment. Prepared by IINAS, EFI and JR," 2014.

[11] Eurostat., "https://ec.europa.eu/eurostat/," [Online].

[12] C. Macharis and Y. M. Bontekoning, "Opportunities for OR in intermodal freight transport research: A review," *European Journal of Operational Research,* vol. 153, no. 2, pp. 400-416, 2004.

[13] M. Janic, "Modelling the full costs of an intermodal and road freight transport network," *Transportation Research Part D-transport and Environment,* vol. 12, no. 1, pp. 33-44, 2007.

[14] K. Brümmerstedt, V. Flitsch and C. Jahn, "Cost Functions in Freight Transport Models," *Operational Excellence in Logistics and Supply Chains,* vol. 22, 2015.

[15] E. Delhaye, T. Breemersch, K. Vanherle, J. Kehoe, M. Liddane and K. Riordan, "The competitiveness of Eropean short-sea freight shipping compared to road and rail transport. COMPASS final report," 2010.

[16] T.-E. S. Hanssen, T. A. Mathisen and F. Jørgensen, "Generalized transport costs in intermodal freight transport," *Procedia - Social and Behavioral Sciences,* vol. 54, pp. 189-200, 2012.

[17] M. Brons and P. Christidis, "External cost calculator for Marco Polo freight transport project proposals – call 2012 version," 2012.

[18] B. V. Herbruggen and S. Logghe, "TREMOVE VERSION 2.3 SIMULATION MODEL FOR EUROPEAN ENVIRONMENTAL TRANSPORT POLICY ANALYSIS," 2005.

[19] B. Tornsjø, "Emissions to air from fishing fleet and sea traffic between Norwegian harbours," Report 2001/6, Statistics Norway, Oslo, 2001.

[20] L. P. Ramos, "The chemistry involved in the steam treatment of lignocellulosic materials," *Química Nova,* vol. 26, no. 6, pp. 863-871, 2003.

[21] A. Duque, P. Manzanares, I. Ballesteros and M. Ballesteros, “Steam Explosion as Lignocellulosic Biomass Pretreatment,” *Biomass Fractionation Technologies for a Lignocellulosic Feedstock Based Biorefinery,* pp. 349-368, 2016.

[22] J. McKechnie, B. Saville and H. L. MacLean, “Steam-treated wood pellets: Environmental and financial implications relative to fossil fuels and conventional pellets for electricity generation,” *Applied Energy,* vol. 180, pp. 637-649, 2016.

[23] P. Wolbers, “Biomass pre-treatment for bioenergy, Case study 4: The steam explosion process technology,” IEA Bioenergy, 2018.

[24] W. H. Mason, *Process and apparatus for disintegration of wood and the like,* 1924.

[25] T. Joronen, P. Björklung and M. Bolhàr-Nordenkampf, “High Quality Fuel by Steam Explosion,” *European Biomass Conference and Exhibition Proceedings,* pp. 1926-1931, 2017.

[26] [Online]. Available: https://www.valmet.com/media/articles/biofuels-and-biomaterials/black-pellets---a-replacement-for-fossil-coal-in-power-plants/.

[27] [Online]. Available: https://www.valmet.com/media/news/press-releases/2018/valmet-to-deliver-the-worlds-first-biotractm-steam-explosion-system-for-black-pellet-production-in-france/.

[28] [Online]. Available: http://biomassmagazine.com/plants/view/7232.

[29] [Online]. Available: https://www.valmet.com/media/news/press-releases/2014/valmet-and-us-based-zilkha-biomass-energy-announce-collaborative-agreement/.

[30] R. P. Overend, E. Chornet and J. A. Gascoigne, “Fractionation of lignocellulosics by steam-aqueous pretreatments,” *Philosophical Transactions of the Royal Society A,* vol. 321, no. 1561, pp. 523-536, 1987.

[31] N. Jacquet, N. Quievy, C. Vanderghem, S. Janas, C. Blecker, J. Devaux, B. Wathelet and M. Paquot, “Influence of steam explosion on the thermal stability of cellulose fibres,” *Polymer Degradation and Stability,* vol. 96, no. 9, pp. 1582-1588, 2011.

[32] P. S. Lam, “Steam explosion of biomass to produce durable wood pellets,” *University of British Columbia PhD Thesis,* 2011.

[33] D. J. Walker, J. Gallagher, A. Winters, A. Somani, S. R. Ravella and D. Bryant, “Process Optimisation of Steam Explosion Parameters on Multiple Lignocellulosic Biomass using Taguchi Method – A Critical Appraisal,” *Frontiers in Energy Research,* vol. 6, no. 46, 2018.

[34] D. E. Priyanto, S. Ueno, K. Hashida and H. Kasai, “Energy-efficient milling method for woody biomass,” *Advanced Powder Technology,* vol. 28, no. 7, pp. 1660-1667, 2017.

[35] H. H. Brownell, E. K. C. Yu and J. N. Saddler, “Steam-explosion pretreatment of wood: Effect of chip size, acid, moisture content and pressure drop,” *Biotechnology and Bioengineering,* vol. 28, no. 6, pp. 792-801, 1986.

[36] M. Ballesteros, I. Ballesteros, M. Negro, J. Oliva, F. Sa´ez and P. Manzanares, “Steam explosion of wheat straw for ethanol production: effect of temperature and time pretreatment and moisture content of biomass,” in *14th European Biomass Conference & Exhibition*, Paris, 2005.

[37] H. Brownell and J. Saddler, “Steam-explosion pretreatment for enzymatic hydrolysis. [US],” *Biotechnol. Bioeng. Symp.; (United States),* 1984.

[38] R. Brusletto and M. Kleinert, *Method of producing carbon-enriched biomass material,* 2014.

[39] G. Garrote, H. Domínguez and J. C. Parajó, “Hydrothermal processing of lignocellulosic materials.,” *European Journal of Wood and Wood Products,* vol. 57, no. 3, pp. 191-202, 1999.

[40] E. Chornet, “Phenomenological kinetics and reaction engineering aspects of steam/aqueous treatments. Steam explosion techniques—fundamentals and industrial applications.,” Gordon and Breach Science Publishers, pp. 21-58, Amsterdam, 1991.

[41] D. Fengel and G. Wegener, Wood: Chemistry, Ultrastructure, Reactions, 1989.

[42] P. Alvira, E. Tomás-Pejó, M. Ballesteros and M. Negro, “Pretreatment technologies for an efficient bioethanol production process based on enzymatic hydrolysis: A review,” *Bioresource Technology,* vol. 101, no. 13, pp. 4851-4861, 2010.

[43] T. Pielhop, J. Amgarten, P. R. v. Rohr and M. H. Studer, “Steam explosion pretreatment of softwood: the effect of the explosive decompression on enzymatic digestibility,” *Biotechnology for Biofuels,* vol. 9, no. 1, pp. 152-152, 2016.

[44] A. K. Biswas, W. Yang and W. Blasiak, “Steam pretreatment of Salix to upgrade biomass fuel for wood pellet production,” *Fuel Processing Technology,* vol. 92, no. 9, pp. 1711-1717, 2011.

[45] M. K. Cieplik, P. Kroon, S. Leiser, P. Abelha and S. Grootjes, “Technical and non-technical requirements and issues to be tackled in WPs,” Arbaheat deliverable D1.2, 2019.

[46] T. Auxenfans, D. Crônier, B. Chabbert and G. Paës, “Understanding the structural and chemical changes of plant biomass following steam explosion pretreatment,” *Biotechnology for Biofuels,* vol. 10, no. 36, 2017.

[47] F. Theuretzbacher, J. Lizasoain, C. Lefever, M. K. Saylor, R. Enguidanos, N. Weran, A. Gronauer and A. Bauer, “Steam explosion pretreatment of wheat straw to improve methane yields: investigation of the degradation kinetics of structural compounds during anaerobic digestion,” *Bioresource Technology,* vol. 179, pp. 299-305, 2015.

[48] M. Negro, P. Manzanares, J. Oliva, I. Ballesteros and M. Ballesteros, “Changes in various physical/chemical parameters of Pinus pinaster wood after steam explosion pretreatment,” *Biomass & Bioenergy,* vol. 25, no. 3, pp. 301-308, 2003.

[49] M. Ibrahim and W. G. Glasser, “Steam-assisted biomass fractionation. Part III : a quantitative evaluation of the clean fractionation concept,” *Bioresource Technology,* vol. 70, no. 2, pp. 181-192, 1999.

[50] S. M. Shevchenko, R. P. Beatson and J. N. Saddler, “The Nature of Lignin from Steam Explosion/Enzymatic Hydrolysis of Softwood,” *Applied Biochemistry and Biotechnology,* vol. 79, pp. 867-876, 1999.

[51] T. P. Schultz, C. J. Biermann and G. D. McGinnis, “Steam explosion of mixed hardwood chips as a biomass pretreatment,” *Industrial & Engineering Chemistry Product Research and Development,* vol. 22, no. 2, pp. 344-348, 1983.

[52] C. Telmo and J. Lousada, “Heating values of wood pellets from different species,” *Biomass & Bioenergy,* vol. 35, no. 7, pp. 2634-2639, 2011.

[53] A. Demirbaş, “Relationships between lignin contents and heating values of biomass,” *Energy Conversion and Management,* vol. 42, no. 2, pp. 183-188, 2001.

[54] H. Shahrukh, A. O. Oyedun, A. Kumar, B. Ghiasi, L. Kumar and S. Sokhansanj, “Net energy ratio for the production of steam pretreated biomass-based pellets,” *Biomass & Bioenergy,* vol. 80, pp. 286-297, 2015.

[55] W. Stelte, “Steam explosion for biomass pre-treatment,” Danish Technological Institute, pp. 1-15, 2013.

[56] M. A. Saeed, N. F. Anez, G. E. Andrews, H. N. Phylaktou and B. M. Gibbs, “Steam exploded pine wood burning properties with particle size dependence,” *Fuel,* vol. 194, pp. 527-532, 2017.

[57] E. Borén, S. H. Larsson, M. Thyrel, A. Averheim and M. Broström, “VOC off-gassing from pelletized steam exploded softwood bark : emissions at different industrial process steps,” *Fuel Processing Technology,* vol. 171, pp. 70-77, 2018.

[58] W. Kaar, C. Gutierrez and C. Kinoshita, “Steam explosion of sugarcane bagasse as a pretreatment for conversion to ethanol,” *Biomass & Bioenergy,* vol. 14, no. 3, pp. 277-287, 1998.

[59] M. E. Mostafa, S. Hu, Y. Wang, S. Su, X. Hu, S. A. Elsayed and J. Xiang, “The significance of pelletization operating conditions: An analysis of physical and mechanical characteristics as well as energy consumption of biomass pellets,” *Renewable & Sustainable Energy Reviews,* vol. 105, pp. 332-348, 2019.

[60] Y. Tang, R. P. Chandra, S. Sokhansanj and J. N. Saddler, “Influence of steam explosion processes on the durability and enzymatic digestibility of wood pellets,” *Fuel,* vol. 211, pp. 87-94, 2018.

[61] N. Kaliyan and R. V. Morey, “Factors affecting strength and durability of densified biomass products.,” *Biomass & Bioenergy,* vol. 33, no. 3, pp. 337-359, 2009.

[62] Z. Liu, A. Quek and R. Balasubramanian, “Preparation and characterization of fuel pellets from woody biomass, agro-residues and their corresponding hydrochars,” *Applied Energy,* vol. 113, pp. 1315-1322, 2014.

[63] W. Stelte, C. Clemons, J. K. Holm, A. R. Sanadi, J. Ahrenfeldt, L. Shang and U. B. Henriksen, “Pelletizing properties of torrefied spruce,” *Biomass & Bioenergy,* vol. 35, no. 11, pp. 4690-4698, 2011.

[64] L. Fele and V. Grilc, “Separation of Furfural from Ternary Mixtures,” *Journal of Chemical & Engineering Data,* vol. 48, no. 3, pp. 564-570, 2003.

[65] W. D. Jong and G. Marcotullio, “Overview of biorefineries based on co-production of furfural, existing concepts and novel developments,” *International Journal of Chemical Reactor Engineering,* vol. 8, no. 1, 2010.

[66] W.-H. Chen, J. Peng and X. T. Bi, “A state-of-the-art review of biomass torrefaction, densification and applications,” *Renewable & Sustainable Energy Reviews,* vol. 44, pp. 847-866, 2015.

[67] Y. Luo, Z. Li, X. Li, X. Liu, J. Fan, J. H. Clark and C. Hu, “The production of furfural directly from hemicellulose in lignocellulosic biomass: A review,” *Catalysis Today,* vol. 319, pp. 14-24, 2019.

[68] S. Sharma, R. Kumar, R. Gaur, R. Agrawal, R. P. Gupta, D. K. Tuli and B. Das, “Pilot scale study on steam explosion and mass balance for higher sugar recovery from rice straw,” *Bioresource Technology,* vol. 175, pp. 350-357, 2015.

[69] G. Marcotullio, W. D. Jong, T. Cardoso and A. Verkooijen, “Bioenergy II: Furfural destruction kinetics during sulphuric acid-catalyzed production from biomass,” *International Journal of Chemical Reactor Engineering,* vol. 7, no. 1, 2009.

[70] G. Machado, S. Leon, F. Santos, R. Lourega, J. Dullius, M. E. Mollmann and P. Eichler, “Literature Review on Furfural Production from Lignocellulosic Biomass,” *Natural Resources,* vol. 7, no. 3, pp. 115-129, 2016.

[71] C. Cara, E. Ruiz, I. Ballesteros, M. J. Negro and E. Castro, “Enhanced enzymatic hydrolysis of olive tree wood by steam explosion and alkaline peroxide delignification,” *Process Biochemistry,* vol. 41, no. 2, pp. 423-429, 2006.

[72] P. Bergman, A. R. Boersma, R. W. R. Zwart and J. H. A. Kiel, “Torrefaction for biomass co-firing in existing coal-fired power stations "BIOCOAL",” *ECN Report ECN-C--05-013,* 2005.

[73] D. Tapasvi, R. Khalil, Ø. Skreiberg, K.-Q. Tran and M. Grønli, “Torrefaction of Norwegian Birch and Spruce: An Experimental Study Using Macro-TGA,” *Energy & Fuels,* vol. 26, no. 8, pp. 5232-5240, 2012.

[74] B. Acharya, I. Sule and A. Dutta, “A review on advances of torrefaction technologies for biomass processing,” *Biomass Conversion and Biorefinery,* vol. 2, no. 4, pp. 349-369, 2012.

[75] J. Wannapeera, B. Fungtammasan and N. Worasuwannarak, “Effects of temperature and holding time during torrefaction on the pyrolysis behaviors of woody biomass,” *Journal of Analytical and Applied Pyrolysis,* vol. 92, no. 1, pp. 99-105, 2011.

[76] V. Repellin, A. Govin, M. Rolland and R. Guyonnet, “Energy requirement for fine grinding of torrefied wood,” *Biomass & Bioenergy,* vol. 34, no. 7, pp. 923-930, 2010.

[77] M. Phanphanich and S. Mani, “Impact of torrefaction on the grindability and fuel characteristics of forest biomass,” *Bioresource Technology,* vol. 102, no. 2, pp. 1246-1253, 2011.

[78] D. Agar and M. Wihersaari, “Bio-coal, torrefied lignocellulosic resources - key properties for its use in co-firing with fossil coal - their status,” *Biomass & Bioenergy,* vol. 44, pp. 107-111, 2012.

[79] S. H. Larsson, M. Rudolfsson, M. Nordwaeger, I. Olofsson and R. Samuelsson, “Effects of moisture content, torrefaction temperature, and die temperature in pilot scale pelletizing of torrefied Norway spruce,” *Applied Energy,* vol. 102, pp. 827-832, 2013.

[80] Q.-V. Bach, K.-Q. Tran, R. A. Khalil, Ø. Skreiberg and G. Seisenbaeva, “Comparative Assessment of Wet Torrefaction,” *Energy & Fuels,* vol. 27, no. 11, pp. 6743-6753, 2013.

[81] E. Sermyagina, J. Saari, J. Kaikko and E. Vakkilainen, “Hydrothermal carbonization of coniferous biomass: Effect of process parameters on mass and energy yields,” *Journal of Analytical and Applied Pyrolysis,* vol. 113, pp. 551-556, 2015.

[82] M. T. Reza, M. H. Uddin, J. G. Lynam and C. J. Coronella, “Engineered pellets from dry torrefied and HTC biochar blends,” *Biomass & Bioenergy,* vol. 63, pp. 229-238, 2014.

[83] S. K. Hoekman, A. Broch, C. Robbins, B. Zielinska and L. Felix, “Hydrothermal carbonization (HTC) of selected woody and herbaceous biomass feedstocks,” *Biomass Conversion and Biorefinery,* vol. 3, no. 2, pp. 113-126, 2013.

[84] B. Erlach, B. Harder and G. Tsatsaronis, “Combined hydrothermal carbonization and gasification of biomass with carbon capture,” *Energy,* vol. 45, no. 1, pp. 329-338, 2012.

[85] V. Dhyani and T. Bhaskar, “A comprehensive review on the pyrolysis of lignocellulosic biomass,” *Renewable Energy,* vol. 129, pp. 695-716, 2017.

[86] V. Sukumar, V. Manieniyan and S. Sivaprakasam, “Bio oil production from biomass using pyrolysis and upgrading - a review,” *International Journal of ChemTech Research,* vol. 8, no. 1, pp. 196-206, 2015.

[87] W. N. R. W. Isahak, M. W. Hisham, M. A. Yarmo and T.-y. Y. Hin, “A review on bio-oil production from biomass by using pyrolysis method,” *Renewable & Sustainable Energy Reviews,* vol. 16, no. 8, pp. 5910-5923, 2012.

[88] A. Bridgwater and G. Peacocke, “Fast pyrolysis processes for biomass,” *Renewable & Sustainable Energy Reviews,* vol. 4, no. 1, pp. 1-73, 2000.

[89] K. H. Kim, I. Y. Eom, S. M. Lee, D. Choi, H. Yeo, I.-G. Choi and J. W. Choi, “Investigation of physicochemical properties of biooils produced from yellow poplar wood (Liriodendron tulipifera) at various temperatures and residence times,” *Journal of Analytical and Applied Pyrolysis,* vol. 92, no. 1, pp. 2-9, 2011.

[90] C. A. Mullen, A. A. Boateng, N. M. Goldberg, I. M. Lima, D. A. Laird and K. B. Hicks, “Bio-oil and bio-char production from corn cobs and stover by fast pyrolysis,” *Biomass & Bioenergy,* vol. 34, no. 1, pp. 67-74, 2010.

[91] K. H. Kim, T.-S. Kim, S.-M. Lee, D. Choi, H. Yeo, I.-G. Choi and J. W. Choi, “Comparison of physicochemical features of biooils and biochars produced from various woody biomasses by fast pyrolysis,” *Renewable Energy,* vol. 50, pp. 188-195, 2013.

[92] J. Rogers and J. G. Brammer, “Estimation of the production cost of fast pyrolysis bio-oil,” *Biomass & Bioenergy,* vol. 36, pp. 208-217, 2012.

[93] K. Weber and P. G. Quicker, “Properties of biochar,” *Fuel,* vol. 217, pp. 240-261, 2018.

[94] H. Abdullah and H. Wu, “Biochar as a Fuel: 1. Properties and Grindability of Biochars Produced from the Pyrolysis of Mallee Wood under Slow-Heating Conditions,” *Energy & Fuels,* vol. 23, no. 8, pp. 4174-4181, 2009.

[95] Q. Hu, H. Yang, D. Yao, D. Zhu, X. Wang, J. Shao and H. Chen, “The densification of bio-char: Effect of pyrolysis temperature on the qualities of pellets,” vol. 200, pp. 521-527, 2016.

[96] S. B. Saleh, J. P. Flensborg, T. K. Shoulaifar, Z. Sárossy, B. B. Hansen, H. Egsgaard, N. DeMartini, P. A. Jensen, P. Glarborg and K. Dam-Johansen, “Release of Chlorine and Sulfur during Biomass Torrefaction and Pyrolysis,” *Energy & Fuels,* vol. 28, no. 6, pp. 3738-3746, 2014.

[97] J. Li, A. Brzdekiewicz, W. Yang and W. Blasiak, “Co-firing based on biomass torrefaction in a pulverized coal boiler with aim of 100% fuel switching,” *Applied Energy,* vol. 99, pp. 344-354, 2012.

[98] F. H. Hedlund, J. Astad and J. Nichols, “Inherent hazards, poor reporting and limited learning in the solid biomass energy sector: A case study of a wheel loader igniting wood dust, leading to fatal explosion at wood pellet manufacturer,” *Biomass & Bioenergy,* vol. 66, pp. 450-459, 2014.

[99] T. Abbasi and S. Abbasi, “Dust explosions–Cases, causes, consequences, and control,” *Journal of Hazardous Materials,* vol. 140, no. 1, pp. 7-44, 2007.

[100] BS 6713-1, “Standard on explosion protection systems: determination of explosion indices of combustible dusts in air, Determination of explosion indices of combustible dusts in air,” BSI, London, 1986.

[101] ISO 6184/1, “International Standards Organization, Explosion Protection Systems, Part 1, Determination of Explosion Indices of Combustible Dusts in Air,” ISO, Geneva, 1985.

[102] BS EN 14034-1, “Determination of explosion characteristics of dust clouds, Part 1: determination of maximum pressure Pmax of dust clouds,” BSI, London, 2004.

[103] BS EN 14034-2, “Determination of explosion characteristics of dust clouds, Part 2: determination of the maximum rate of explosion pressure rise of dust clouds,” BSI, London, 2006.

[104] BS EN 14034-3, “Determination of explosion characteristics of dust clouds, Part 3: determination of the lower explosion limit LEL of dust clouds,” BSI, London, 2006.

[105] P. McNamee, L. Darvell, J. Jones and A. Williams, “The combustion characteristics of high-heating-rate chars from untreated and torrefied biomass fuels,” *Biomass & Bioenergy,* vol. 82, pp. 63-72, 2015.

[106] C. H. Medina, H. Sattar, H. N. Phylaktou, G. E. Andrews and B. M. Gibbs, “Explosion reactivity characterisation of pulverised torrefied spruce wood,” *Journal of Loss Prevention in The Process Industries,* vol. 36, pp. 287-295, 2015.

[107] J. S. Tumuluru, C. T. Wright, R. D. Boardman, N. A. Yancey and S. Sokhansanj, “A Review on Biomass Classification and Composition, Co-firing Issues and Pretreatment Methods,” in *2011 ASABE Annual International Meeting, Louisville, Kentucky, 7-10 August 2011*, 2011.

[108] P. Basu, J. Butler and M. A. Leon, “Biomass co-firing options on the emission reduction and electricity generation costs in coal-fired power plants,” *Renewable Energy,* vol. 36, no. 1, pp. 282-288, 2011.

[109] C. Ndibe, S. Grathwohl, M. Paneru, J. Maier and G. Scheffknecht, “Emissions reduction and deposits characteristics during cofiring of high shares of torrefied biomass in a 500 kW pulverized coal furnace,” *Fuel,* vol. 156, pp. 177-189, 2015.

[110] G. Yildiz, F. Ronsse, R. Venderbosch, R. v. Duren, S. R. Kersten and W. Prins, “Effect of biomass ash in catalytic fast pyrolysis of pine wood,” *Applied Catalysis B-environmental,* vol. 168, no. 169, pp. 203-211, 2015.

[111] E. Agbor, X. Zhang and A. Kumar, “A review of biomass co-firing in North America,” *Renewable & Sustainable Energy Reviews,* vol. 40, pp. 930-943, 2014.

[112] E. Rokni, X. Ren, A. Panahi and Y. A. Levendis, “Emissions of SO2, NOx, CO2, and HCl from Co-firing of coals with raw and torrefied biomass fuels,” *Fuel,* vol. 211, pp. 363-374, 2018.

[113] M. Pronobis, “Evaluation of the influence of biomass co-combustion on boiler furnace slagging by means of fusibility correlations,” *Biomass & Bioenergy,* vol. 28, no. 4, pp. 375-383, 2005.

[114] M. Sami, K. Annamalai and M. Wooldridge, “Co-firing of coal and biomass fuel blends,” *Progress in Energy and Combustion Science,* vol. 27, no. 2, pp. 171-214, 2001.

[115] B. Jenkins, L. Baxter and T. Miles, “Combustion properties of biomass,” *Fuel Processing Technology,* vol. 54, no. 1, pp. 17-46, 1998.

[116] S. Munir, W. Nimmo and B. M. Gibbs, “Co-combustion of Agricultural Residues with Coal: Turning Waste into Energy,” *Energy & Fuels,* vol. 24, no. 3, pp. 2146-2153, 2010.

[117] P. Grammelis, G. Skodras and E. Kakaras, “Effects of biomass co-firing with coal on ash properties. Part I: Characterisation and PSD,” *Fuel,* vol. 85, no. 16, pp. 2310-2315, 2006.

[118] A. T. Masiá, B. Buhre, R. Gupta and T. Wall, “Characterising ash of biomass and waste,” *Fuel Processing Technology,* vol. 88, no. 11, pp. 1071-1081, 2007.

This project has received funding from the European Union’s Horizon 2020
research and innovation programme under grant agreement No 818349